REPORT DOCUMENTATION PAGE

Form Approved
OMB No. 0704-0188

1. AGENCY USE ONLY (Leave blank)	2. REPORT DATE	3. REPORT TYPE AND DATES COVERED
		Final Technical 01 June 1992 - 30 November 1995

4. TITLE AND SUBTITLE

Joint Research on Computational Fluid Dynamics and Fluid Flow Control

5. FUNDING NUMBERS

G - F49620-92-J-0279

6. AUTHOR(S)

J.S. Gibson

7. PERFORMING ORGANIZATION NAME(S) AND ADDRESS(ES)

University of California, Los Angeles
Mechanical and Aerospace Engineering Department
38-137 Engr. IV, Box 159710
Los Angeles, California 90095-1597

AFOSR-TR-96

0216

9. SPONSORING/MONITORING AGENCY NAME(S) AND ADDRESS(ES)

AFOSR/NA
110 Duncan Avenue, Suite B115
Bolling AFB, DC 20332-0001

10. SPONSORING/MONITORING AGENCY REPORT NUMBER

11. SUPPLEMENTARY NOTES

12a. DISTRIBUTION/AVAILABILITY STATEMENT

Approved for limited public release; distribution is unlimited.

12b. DISTRIBUTION CODE

13. ABSTRACT (Maximum 200 words)

This research project has developed methods for computational fluid dynamics and fluid-flow control. The research on computational fluid dynamics has consisted of the analysis and development of simulations and mathematical models of two-dimensional fluid motion. The control research has used a hierarchy of simulations and models t design feedback controllers for fluid flows. Both adaptive and nonadaptive controllers were developed. The research was motivated by the need to stabilize high-Reynolds number flows around bodies such as delta-wing aircraft.

14. SUBJECT TERMS

computational fluid dynamics; flow control; vortex models; finite difference scheme; adaptive control; feedback control; nonlinear control

15. NUMBER OF PAGES

44

16. PRICE CODE

17. SECURITY CLASSIFICATION OF REPORT	18. SECURITY CLASSIFICATION OF THIS PAGE	19. SECURITY CLASSIFICATION OF ABSTRACT	20. LIMITATION OF ABSTRACT
Unclassified	Unclassified	Unclassified	UL

GENERAL INSTRUCTIONS FOR COMPLETING SF 298

The Report Documentation Page (RDP) is used in announcing and cataloging reports. It is important that this information be consistent with the rest of the report, particularly the cover and title page. Instructions for filling in each block of the form follow. It is important to ***stay within the lines*** to meet ***optical scanning requirements***.

Block 1. Agency Use Only *(Leave blank)*.

Block 2. Report Date. Full publication date including day, month, and year, if available (e.g. 1 Jan 88). Must cite at least the year.

Block 3. Type of Report and Dates Covered. State whether report is interim, final, etc. If applicable, enter inclusive report dates (e.g. 10 Jun 87 - 30 Jun 88).

Block 4. Title and Subtitle. A title is taken from the part of the report that provides the most meaningful and complete information. When a report is prepared in more than one volume, repeat the primary title, add volume number, and include subtitle for the specific volume. On classified documents enter the title classification in parentheses.

Block 5. Funding Numbers. To include contract and grant numbers; may include program element number(s), project number(s), task number(s), and work unit number(s). Use the following labels:

C	- Contract	PR	- Project
G	- Grant	TA	- Task
PE	- Program Element	WU	- Work Unit Accession No.

Block 6. Author(s). Name(s) of person(s) responsible for writing the report, performing the research, or credited with the content of the report. If editor or compiler, this should follow the name(s).

Block 7. Performing Organization Name(s) and Address(es). Self-explanatory.

Block 8. Performing Organization Report Number. Enter the unique alphanumeric report number(s) assigned by the organization performing the report.

Block 9. Sponsoring/Monitoring Agency Name(s) and Address(es). Self-explanatory.

Block 10. Sponsoring/Monitoring Agency Report Number. *(If known)*

Block 11. Supplementary Notes. Enter information not included elsewhere such as: Prepared in cooperation with...; Trans. of...; To be published in.... When a report is revised, include a statement whether the new report supersedes or supplements the older report.

Block 12a. Distribution/Availability Statement. Denotes public availability or limitations. Cite any availability to the public. Enter additional limitations or special markings in all capitals (e.g. NOFORN, REL, ITAR).

- DOD - See DoDD 5230.24, "Distribution Statements on Technical Documents."
- DOE - See authorities.
- NASA - See Handbook NHB 2200.2.
- NTIS - Leave blank.

Block 12b. Distribution Code.

- DOD - Leave blank.
- DOE - Enter DOE distribution categories from the Standard Distribution for Unclassified Scientific and Technical Reports.
- NASA - Leave blank.
- NTIS - Leave blank.

Block 13. Abstract. Include a brief *(Maximum 200 words)* factual summary of the most significant information contained in the report.

Block 14. Subject Terms. Keywords or phrases identifying major subjects in the report.

Block 15. Number of Pages. Enter the total number of pages.

Block 16. Price Code. Enter appropriate price code *(NTIS only)*.

Blocks 17. - 19. Security Classifications. Self-explanatory. Enter U.S. Security Classification in accordance with U.S. Security Regulations (i.e., UNCLASSIFIED). If form contains classified information, stamp classification on the top and bottom of the page.

Block 20. Limitation of Abstract. This block must be completed to assign a limitation to the abstract. Enter either UL (unlimited) or SAR (same as report). An entry in this block is necessary if the abstract is to be limited. If blank, the abstract is assumed to be unlimited.

ABSTRACT

This research project has developed methods for computational fluid dynamics and fluid-flow control. The research on computational fluid dynamics has consisted of the analysis and development of simulations and mathematical models of two-dimensional fluid motion. The control research has used a hierarchy of simulations and models to design feedback controllers for fluid flows. Both adaptive and nonadaptive controllers were developed. The research was motivated by the need to stabilize high-Reynolds number flows around bodies such as delta-wing aircraft.

FINAL TECHNICAL REPORT

AFOSR GRANT F49620-92-J-0279
Joint Research on Computational Fluid Dynamics and Fluid Flow Control

J.S. Gibson
Mechanical and Aerospace Engineering
University of California, Los Angeles 90095-1597

1 Introduction

Objectives and Approach. The basic objective of the research project was the integrated development of methods for feedback control of fluid flows and methods for efficient numerical simulation of flow properties that are most important for controller design and verification. In control design, the objective is a strategy for adaptive feedback control of the highly nonlinear vortex dynamics characteristic of flow past bluff bodies. In computational fluid dynamics, the objective is specialized vortex methods for long-time simulation of actively controlled flows.

The project has developed coordinated methods for computational fluid dynamics (CFD) and flow control. The CFD research has consisted of the analysis and development of computational simulations and mathematical models for solving problems of two-dimensional fluid motion. The control research has used the hierarchy of simulations and models to design controllers for fluid flows. The research was motivated by the need to stabilize high-Reynolds number flows around bodies such as delta-wing aircraft.

A hierarchy of models were constructed to facilitate the control design for the problem of stabilizing vortices behind a flat plate. The models used were a point-vortex simulation, a vortex blob simulation, and a finite difference simulation of the full Navier-Stokes equations. The point-vortex model [1] facilitated the use of mathematical analysis and analytic control design, the point-vortex and vortex blob simulations were of sufficient computational efficiency that adaptive identification and adaptive control procedures could be developed [2, 3, 4], and the finite difference simulation was created for the validation of our identification and control procedures.

Main Results. The most important results of the project deal with control of flows with large vortical structures. These main results are:

- Effective adaptive regulation of the oscillations in measured cross-stream velocity in a wake typical of flow past bluff bodies [2, 4] [1];
- Adaptive identification of input/output models that reveal the effect of relative actuator/sensor locations on the zero dynamics of the nonlinear input/output map of the flow field [3, 4];
- Use of a reduced-order vortex model to design a nonlinear controller that stabilizes the large vortical structures in flow past a plate, as simulated by a very high-order CFD model [1];
- Design of an effective fixed-gain linear controller that uses a realistic point velocity measurement and stabilizes the large vortical structures in flow past a plate [3, 4];

An important distinguishing feature of this is the fact that most of the controllers are based on digital input/output models, which usually are identified from input/output data. This means that the control methods should be applicable to more complicated flows with qualitative features similar to those of the simulation models. Also, the input/output models used assume *realistic* sensor measurements, such as point velocity measurements near the surface of a body. Because adaptive control based on an identified input/output model has proved successful in stabilizing the oscillating cross-stream velocity in the vortical flow generated by the vortex-blob model used in [2, 3, 4], we plan to continue to develop adaptive control methods for various classes of vortical flows. However, in our recent work on flow control, we have not used adaptive control exclusively; we have also used non-adaptive linear and nonlinear control.

The relevance of adaptively identified linear input/output models for control of highly nonlinear fluid flows is demonstrated in [2, 3]; however, preliminary simulation results during the current project indicate that, for some important flows, a nonlinear input/output model should serve better as the basis for controller design. Future research is planned to pursue the use of nonlinear time series in control of fluid flows. Both adaptive and nonadaptive controllers should be studied. The reduced-order vortex models should provide insight about which nonlinear terms to include in time-series models.

[1] The papers [1], [2], [3] are included in the Appendix of this report.

2 Modeling and Identification for Control

2.1 Linear Input/Output Models

The adaptive (and quasi adaptive) controllers used for flow control have been based on either linear or nonlinear digital input-output models. The linear input-output models, often referred to as ARX (Auto-Regressive with eXogenous inputs) models have the form

$$y(t) = \sum_{i=1}^{n} A_i(t)y(t-i) + \sum_{i=1}^{n} B_i(t)u(t-i) \tag{2.1}$$

where $y(t)$ is the vector of measured outputs and $u(t)$ is the vector of control inputs. The matrices $A_i(t)$ and $B_i(t)$ are time-varying coefficients to be identified adaptively from input/output data. Although the high-Reynolds flows that we have controlled are highly nonlinear, our recent research has demonstrated that linear ARX models can serve as the basis for adaptive controllers for such flow because the adaptive identification scheme achieves a local linearization of the true nonlinear input/output map of the flow field.

The results in [2, 4] demonstrated the ability of an adaptive controller based on a linear ARX model to reduce the amplitude of oscillation in a wake typical of those generated by flow past bluff bodies. A study in [3, 4] of the zero dynamics of the nonlinear vortex-blob model of the flow field and of the zero dynamics of the adaptively identified linear ARX model shows that the ARX model captures an important effect of actuator and sensor locations on the stability of the zero dynamics. The adaptively identified model had all stable zeros when the actuator was downstream of the sensors, while this model had some unstable zeros whenever the actuator was upstream of the sensors; i.e., the identified linear model was minimum phase if and only if the sensors were upstream of the actuator. It is well known that whether a plant is minimum phase is an important issue in determining whether feedback controllers can produce closed-loop stability and robustness. In particular, a controller that somehow inverts the plant produces an unstable closed-loop system when the plant is nonminimum phase. That the identified unstable zeros of the linear input/output model represented actual and important characteristics of the flow field was verified as discussed in [3, 4] by simulation of a nonlinear feedback control based on the true, explicit vortex-blob model; in this simulation, as predicted by the identified ARX model, the closed loop-system was either stable or unstable depending on whether the actuator was downstream or upstream of the sensors.

That sensors located upstream of actuators produce a minimum-phase plant for the particular flow-control problem in [3] suggests that, as should be expected in light of experience with flexible structures and other classes of control systems, stability of zero dynamics in many flow-control problems depends on the relationship between actuator and sensor locations. However, the form of this dependence will vary for different flows, bluff bodies, and actuators and sensors. This will be a major issue in future research, especially when we employ multiple actuators and sensors and controllers based on nonlinear time series. Any results that can guide actuator/sensor placement to produce minimum-phase plants will be useful for any approaches to flow control, not just the control designs that we use.

2.2 Nonlinear Input/Output Models

Although we have been successful in basing adaptive feedback controllers for certain nonlinear fluid flows on linear input/output models with adaptively varying coefficients, we have preliminary simulation results indicating that nonlinear input/output models (i.e. *nonlinear time series*) can be more accurate prediction models for adaptive control of fluid models. The nonlinear time series models that we have considered have the form

$$y(t) = \sum_{i=1}^{n} A_i(t)y(t-i) + \sum_{i=1}^{n} B_i(t)u(t-i) + \sum_{i=1}^{n}\sum_{j=1}^{m} A_{ij}(t)f_j(y(t-i)) + \sum_{i=1}^{n}\sum_{j=1}^{k} B_{ij}(t)g_j(u(t-i)) \tag{2.2}$$

where y is a measured output vector and u is a control vector. The functions f_j and g_j can be anything from multivariable polynomials to radial basis functions to splines or perhaps wavelets. Recently, there has been considerable research on using nonlinear time series to model the input/output characteristics of highly nonlinear, often chaotic systems, particularly, fluid dynamics [5, 6, 7, 8], [9, 10, 11]. We believe that the reduced-order point-vortex model that Cortelezzi has used recently for design of nonlinear controllers can be used to determine good candidates for the functions f_j and g_j in the nonlinear time series on which adaptive flow controllers are based.

We identify the coefficient matrices $A_i(t)$, $B_i(t)$, $A_{ij}(t)$, and $B_{ij}(t)$, whereas the approach taken by previous researchers on nonlinear time series has been to generate long sequences of input/output data from a nonlinear plant and then use off-line least-squares parameter identification to determine constant coefficient matrices A_{ij} and B_{ij} for a model of the form (2.2). This approach is based on the questionable assumption that a single nonlinear model can approximate the input/output map for a nonlinear system in all regions of state space. Our approach allows the time series used to approximate the input/output map to vary adaptively as the state of the nonlinear system moves in state space. We have had considerable success with this approach in control of simulations of fluid flows and related nonlinear systems [12, 13, 2, 14], even though we have restricted the time series used so far for control design to be linear. Some of our preliminary simulations comparing adaptively varying linear and nonlinear time series for output prediction suggest that at least modest improvement can be achieved by including polynomial nonlinearities in the time series. We have carried out such comparisons on vortex simulations and on the Lorentz equations.

2.3 Phase Space Analysis of Vortex-blob and Point-vortex Models

While the input/output models have been prominent in the control design and analysis, we also have used the point-vortex model in design of nonlinear controllers. This nonlinear state-space model is a reduced-order approximation to the high-order vortex-blob model. Because the point-vortex model is based explicitly on the physics of vortical flow, it allows important physical information to be incorporated into controller design, whereas the input/output models sometimes miss relevant physics.

The application of a controller derived for a low-dimensional (reduced) model to a model of higher or of infinite dimension is not trivial. Besides trial-and-error, a better and more

scientific approach is to prove or to verify that the two systems are dynamically equivalent; i.e., that the phase spaces of the low-dimensional system and the high-dimensional system are topologically equivalent. If the two systems are dynamically equivalent, then the controller designed for the reduced model should be able to control the higher-order model. If, instead, the two systems are not dynamically equivalent, then analyzing the differences between the structures of their respective phase spaces should provide the information necessary to modify the controller for the reduced model to enable it to control the high-order system.

In our research, the controller derived for the reduced point-vortex model predicts the suction necessary to confine the wake when the position and strength of the vortex pair is known. To apply this controller to the vortex blob simulation, we need, first of all, to define a quantity that we call the *center of circulation*, which represents the ensemble of vortex blobs. The position of the center of circulation can be fed back to several classes of controllers.

The center of circulation must conserve the total circulation to satisfy Kelvin's theorem and at least the first moment, the linear impulse, of the ensemble. We define the total circulation as

$$\Gamma_C = \sum_{i=1}^{N} \Gamma_i, \tag{2.3}$$

and the linear impulse of the ensemble as

$$I_C = \left(\zeta_C - \frac{1}{\bar{\zeta}_C}\right) = \sum_{i=1}^{N} I_i = \sum_{i=1}^{N} \Gamma_i \left(\zeta_i - \frac{1}{\bar{\zeta}_i}\right), \tag{2.4}$$

where ζ_i is the position in the mapped plane of the blob of strength Γ_i. The above equation permits us to derive the position of the center of circulation of an ensemble of vortices in the presence of a body of finite size. We have:

$$\zeta_C = \sqrt{\frac{I_C}{\bar{I}_C}} \left[\frac{\sqrt{I_C \bar{I}_C + 4a^2\Gamma_C^2} + \sqrt{I_C \bar{I}_C}}{2\Gamma_C} \right]. \tag{2.5}$$

Hence, the center of circulation can be envisioned as a point vortex of circulation Γ_C positioned at ζ_c. Note in the case of continuously distributed vorticity is possible to derive a equivalent integral definition of the center of circulation.

The proof of the dynamic equivalence of the point-vortex and the vortex-blob models can be given deriving the equation of motion for the center of circulation, and showing that the phase space associated with the dynamics of the center of circulation is topologically equivalent to the phase space associated with the dynamics of the point vortex. Although non trivial, the derivation of the equation of motion for the center of circulation is, in principle, possible. Since the position and the strength of the center of circulation are defined in terms of positions and circulations of the all the vortex blobs in the ensemble, it should be possible to derive the equation of motion for the center of circulation from the equations of motion of the vortex blobs. When the equation of motion for the center circulation is available it can be analyzed as a dynamical system computing fixed points, limit cycles, etc. and studying their structure and their stability. The final step of this

process is the construction of the phase space associated with the dynamics of the center of circulation and the comparison with the phase space associated with the dynamics of the point vortex. If the phase spaces of the two systems present the same types of fixed points, limit cycles, etc. in the region of the phase space of interest in the application under consideration then the controller derived for the reduced model should, in principle, be able to govern the dynamics of the higher order system.

A less formal approach, the one taken up to now in our current research, is the numerical verification of the equivalence of the phase spaces. In this case the controller derived for the reduced model is applied to the higher order model and has to be able to govern some of the dynamics of higher order model. To verify the equivalence of the phase spaces one should run a series of numerical experiments to confirm that the controller is able to drive the system, for example, near to a stable fixed point of the reduced model. The numerical experiments are, of course, suggested by the knowledge of the phase space of the reduced model. A methodical reconstruction of the phase plane of the higher order model would provide crucial information about performance and limitation of the controller and possible suggestions in the case the controller has to be redesigned.

3 Active Control of Flow Past a Plate

3.1 Background

In recent years, efforts to modify certain features of the wake behind bluff and slender bodies have been successful. The objectives of such efforts have been reduction or magnification of the wake thickness [15], wake stabilization [16], vortex cancellation [17], pattern reproduction [18], [19], [20], and lift enhancement [21], [22]. In all these investigations, the free-stream velocity was kept constant, and quasi-steady results were achieved usually by moving the body or the actuator with a frequency scaled by the shedding frequency. In a more general situation, in which the free-stream velocity is time dependent, this approach is generally not sufficient to control the flow.

The problem of actively controlling an unsteady fluid flow is in general nonlinear. Control of nonlinear systems is still a subject of much research, and there is no reliable method to obtain a controller for a highly nonlinear infinite-dimensional system like a fluid flow with vortical structures. It is well known that the model chosen to represent the plant is of crucial importance in the derivation of the controller. A very complex and detailed model, the full Navier-Stokes equations, for example, might generate an overly complex controller or might make the derivation of the controller impossible. On the other hand, an over-simplified or linear model facilitates the derivation of a controller but might generate a controller unable to achieve the desired control objective. A reasonable compromise is a reduced model able to capture the dynamic features of the flow that one wants to control. See [23] [24] [25]. Typically, the reduced model is a low-dimensional system governed by a set of ordinary differential equations, while the real flow has infinite dimension. An advantage of working with a reduced model is that one can use dynamical system analysis to investigate the problem. Analysis of the phase space of the reduced system should provide information about fixed points, limit cycles, bifurcation points, etc., and consequently should provide information about effectiveness and robustness of a controller. Another advantage of model reduction is the potential for producing fast numerical algorithms, which are essential for controlling a real flow.

Before attempting to control a laboratory flow, one should take the intermediate step of controlling the same class of flows simulated by a more sophisticated CFD (Computational Fluid Dynamics) code. The application of the controller derived for the reduced model to a complex model should be successful if the two models are dynamically equivalent; i.e., if the phase spaces of the two models are topologically equivalent. The equivalence of the two models can be investigated via dynamical system and time series analysis. There are many advantages in controlling a flow simulated by another CFD code. All the flow quantities necessary to feedback to the controller can be easily measured. The action of the controller is automatically synchronized with the evolution of the flow because both algorithms run in virtual time. Furthermore, the controller can be tested on gradually more complex flows. For example, a controller derived first for an inviscid vortex-blob model can be applied to a slightly viscous finite-difference model of the same flow and, if necessary, the controller can be modified to handle the more realistic model. Finally, the control of a laboratory flow can be attempted when the controller generated by this chain of refinements is robust enough to perform in the presence of the unmodeled and unpredictable uncertainties affecting the real system and is fast enough to control the flow in real time. Such an interative design

procedure is required to produce a controller able to handle the flow governed by the Navier-Stokes equations.

3.2 Control of the Wake behind a Flat Plate

Active control of flow past a thin, flat plate perpendicular to the free-stream velocity in an unsteady flow is the focus of our most recent research. (See Figure 1.) Although simplified, this problem contains most of the difficulties associated with control of the unsteady separated flows past bluff bodies. Manipulating and stabilizing the wake past a plate is closely related to important aeronautical applications: lift enhancement, drag reduction, fluid-structure interaction, vortex management. We also choose this geometry because the flow creates a wake dominated by large coherent vortical structures in a large regime and because it permits us to study the problem theoretically using a reduced model, as well as numerically with several types of CFD models.

In the simplest model, we represent the unsteady separation from the tips of a flat plate by means of a pair of point vortices whose time-dependent circulation is predicted by an unsteady Kutta condition. The motion of the vortex pair is determined by a non-linear ordinary differential equation first proposed by Brown and Michael [26]. A suitable vortex shedding mechanism is also introduced to allow the simulation of flows involving multiple vortices. This reduced model captures the main features of the flow and, for example, is quite accurate for power-law starting flows. See Section 2 of [1] [2] for a detailed discussion.

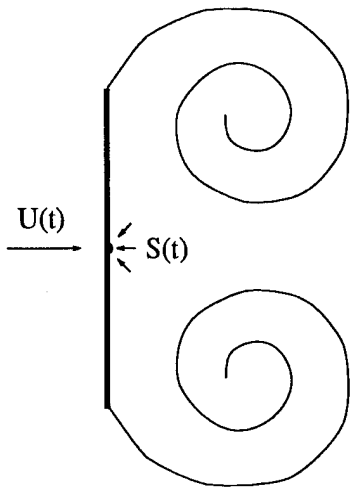

Figure 1: Unsteady separated flow past a plate. Vortex sheets are shown. Free-stream velocity = $U(t)$, Suction = $S(t)$.

The control actuator is a suction point placed on the downstream wall of the plate. As indicated in Figure 1, the strength of the time-dependent suction is $S(t)$. The control objective is to confine the wake to a single vortex pair of constant circulation. We show that suction, as mean of control, is very effective in this type of problem. For any time-dependent

[2]The papers [1], [2], and [3] are included in the Appendix of this report.

free-stream velocity in the point-vortex model, the Kutta condition determines the suction necessary to inhibit the production of additional circulation when a vortex pair is present in the flow. Thus the closed-form feedback control law can be determined analytically from the Kutta condition. (See Section 3 of [1] in the Appendix of this report.)

We perform a dynamical system type of analysis to characterize the performance of the controller. When the free-stream is constant, we show the existence of fixed points for the unperturbed system and compute the locus of the fixed points. There is a critical value for the circulation associated with the vortex pair above which one can find two pairs of fixed points: a pair of stable nodes and a pair of saddle points farther downstream. The circulation plays the role of a bifurcation parameter and the vector field undergoes to a saddle-node bifurcation when the circulation is near its critical value. The analysis of the phase space shows the existence of a controllable region between the plate and the stable manifolds of the saddle points. When the free-stream velocity oscillates periodically about a unit mean, we compute the Poincaré section to characterized the perturbed system. We show the topological equivalence between the Poincaré section and the phase space of the unperturbed system. The stable node of the Poincaré section represents a limit cycle while the saddle point represents an unsteady periodic orbit. See Section 4 of [1] in the Appendix for a detailed discussion.

3.3 High-Order Simulation

The second step of our research on controlling the flow past a plate is to apply the controller derived for the (low-order) point-vortex model to the high-order vortex-blob model and compare the performance of the same controller applied to the two different models. We use a vortex-blob model as an intermediate step before attempting the control of the flow simulated by the Navier-Stokes equations because complexity of the flow simulated by the vortex blob model, although three orders of magnitude higher than the reduced model, is still finite. To complete the final step of controlling the Navier-Stokes equations for this problem, we currently are in the process of developing the finite-difference simulation.

In the vortex-blob model, the unsteady separation from the tips of a plate is simulated by introducing at each time step a new vortex blob in the flow to satisfy the Kutta condition. The motion of the vortex blobs is determined by a set of nonlinear differential equations. The number of equations to be solved increases in time as new vortex blobs are introduced in the flow. For the simulations discussed here, the point-vortex model has two states; the vortex-blob model has a variable number of states that grows to more than 2000.

The controller derived for the reduced model predicts the suction necessary to confine the wake when the position an strength of the point vortex is known. To apply this controller to the vortex blob simulation we define a quantity, the center of circulation, to represent the ensemble of vortex blobs. The center of circulation can be envisioned as a point vortex which conserves circulation and linear impulse of the ensemble. The position and the circulation of the center of circulation is fed back to the controller closing the feedback loop.

We have applied the controller derived for the reduced model to the vortex blob model using the concept of *center of circulation.* To support this step, we verified numerically the dynamical equivalence of the two models; i.e., the topological equivalence of the phase spaces of the two models. Using a family of free-stream conditions we produced vortical

structures of different circulation and verified that the center of circulation is driven very near the fixed point of the reduced model. We also verified that nearly the same critical value of circulation exists for the vortex-blob model.

We compare the performance of the controller based on the Kutta condition when applied to the reduced (point-vortex) model and to the vortex-blob model. In both simulations the same free-stream velocity is used. It increases from rest, reaches a maximum value, and decreases to a final constant value at $t = 1$, as shown in Figure 2. During the deceleration, the rate of circulation production changes sign triggering the controller, as shown in Figure 5. Figure 3 shows the comparison between the trajectory of the point vortex and the trajectory of the center of circulation. These trajectories are nearly the same and both, point vortex and center of circulation, are driven to nearly the same fixed point. The comparison between the total circulation of the top point vortex and of the top center of circulation is also satisfactory. The controller works, of course, perfectly with the point-vortex model, but the controller also drives circulation of the vortex blob simulation closed to the predicted value (Figure 4). It is interesting to compare the control signal, (i.e., the suction) as function of time. Figure 5 shows that the suction is nearly the same for the two simulations during the first quarter of the time interval, then the suction for the vortex-blob model deviates about 20%, but finally recovers.

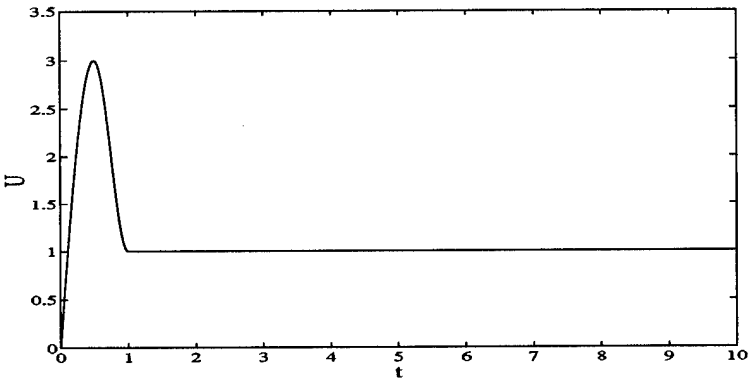

Figure 2: Free-stream velocity $U(t)$.

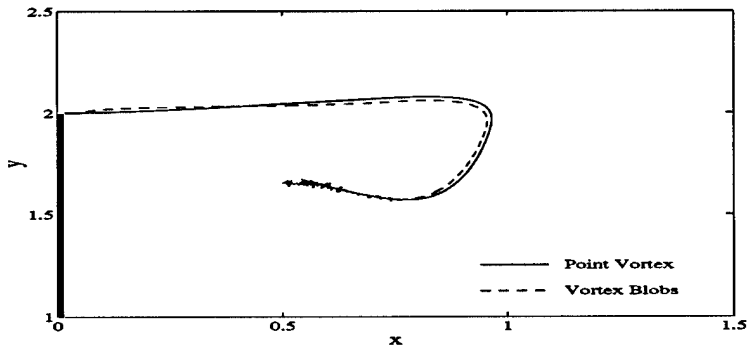

Figure 3: The trajectory of the point vortex in the reduced model and the trajectory of the center of circulation in the vortex-blob model.

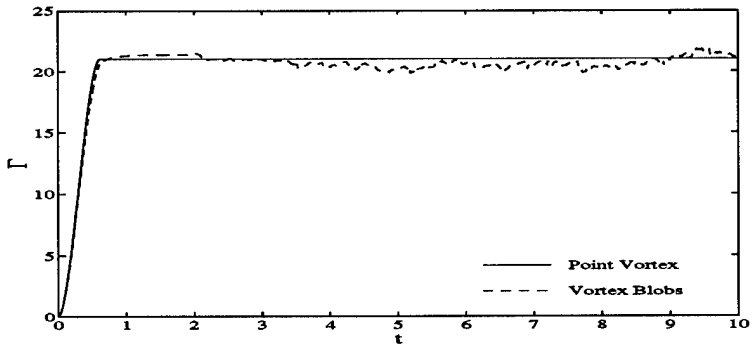

Figure 4: Top vortex circulation $\Gamma(t)$: comparison between point-vortex model and vortex-blob model.

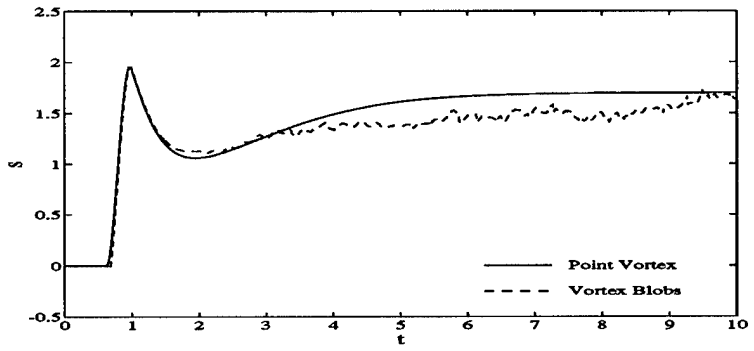

Figure 5: Control suction $S(t)$: comparison between point-vortex model and vortex-blob model.

Figure 6 presents a comparison between the stream function of the two simulations at different times during the capture of the vortex pair. The two simulations differ in the symmetry condition: no symmetry condition was imposed on the vortex-blob simulation while the point-vortex simulation is constrained to be symmetric. However, the flow field generated by the vortex-blob simulation is almost exactly symmetric, so only the top half of the domain is shown. Figure 6(a)–(d) show the flow at time $t < t_s$, where two recirculating bubbles grow and merge together. As suction becomes non-zero, the recirculating bubble splits into two bubbles, as shown in Figure 6(e) and (f). Figure 6(e)–(l) show how the vortex and the center of circulation are driven to the respective fixed points. Figure 6(i)–(l) are nearly identical because the flow has almost reached the steady state.

We emphasize that the point-vortex simulation involves only 2 vortices while the vortex-blob simulation involves about 1000 blobs. The simulations are remarkably similar; only the size of the vortex core, in black, is clearly different. In the vortex-blob simulation the vortex core occupies a large part of the recirculation region due to the distribution of blobs in the region, while in the point-vortex simulation the stream function has a sharp peak at the location of the point vortex.

We emphasize also that the same controller was applied to both the point-vortex simulation and the vortex-blob simulation. In view of the large differences between the two numerical models, we believe that the remarkable agreement between the two simulations suggests strongly that the same controller should be successful on an even more realistic finite-difference simulation and, ultimately, on an experimental flow.

It is important to note that we have quite recent results for a different controller for this same problem. This latest controller uses proportional and integral (PI) feedback of the position of the center of circulation, but it does not use the Kutta condition or any other internal information about the flow. This controller gives results on the vortex-blob simulation almost identical to those produced by the controller based on the Kutta condition. The success of this PI controller leads us to believe that we will be successful in applying other control designs based on input/output models to this class of flows.

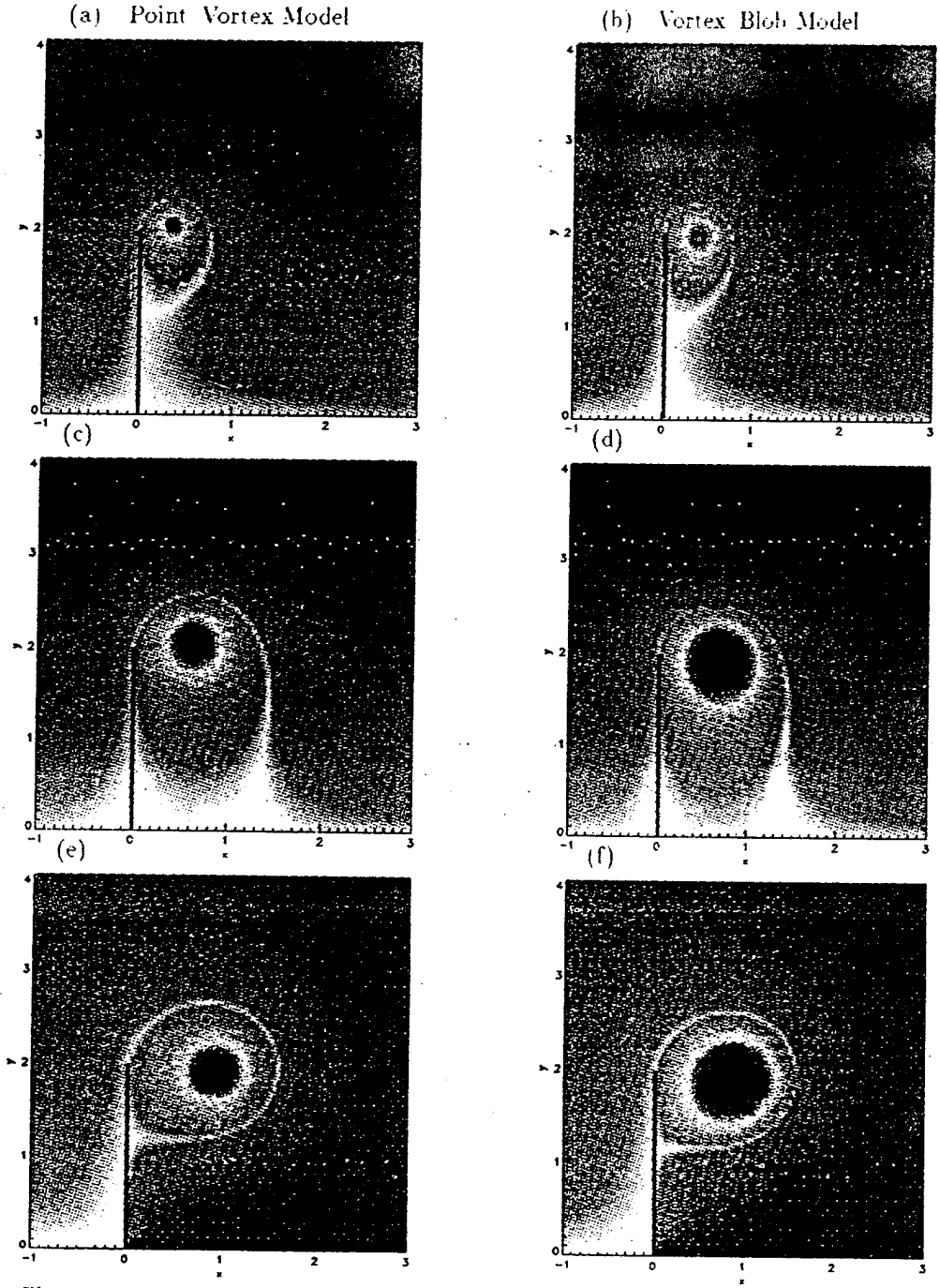

Figure 6: Instantaneous stream function: t=0.4(a),(b); t=0.6(c),(d); t=1.0(e),(f).

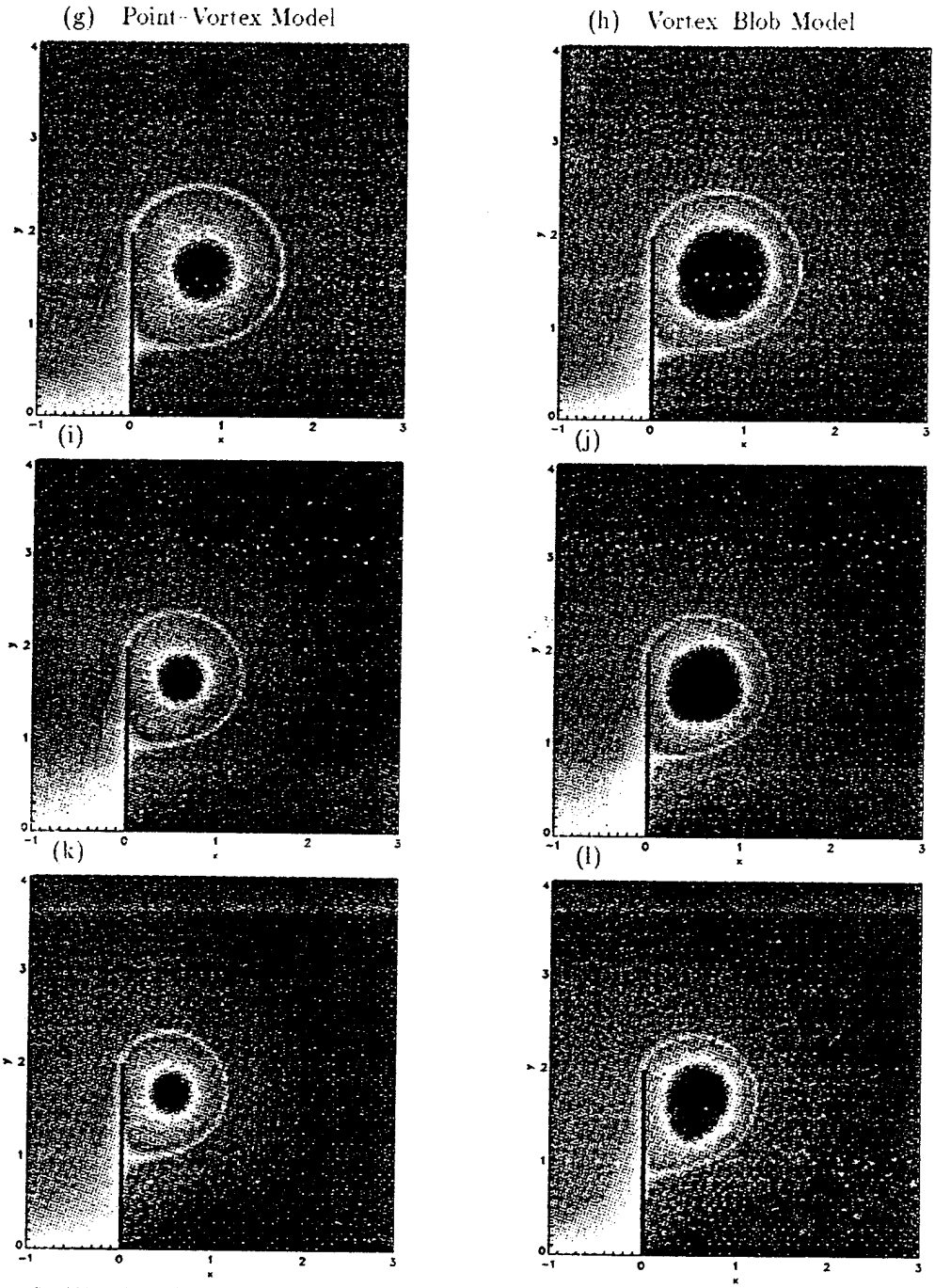

Figure 6: (Continued) Instantaneous stream function: t=2.0(g),(h); t=4.0(i),(j); t=8.0(k),(l).

References

[1] L. Cortelezzi, "On the active control of the wake past a plate with a suction point on the downstream wall," *Journal of Fluid Mechanics*. Submitted.

[2] C.R. Anderson, H.-L. Chang, and J.S. Gibson, "Adaptive control of vortex dynamics," in *IEEE Conference on Decision and Control*, (San Antonio, TX), IEEE, December 1993.

[3] C.R. Anderson, H.-L. Chang, and J.S. Gibson, "Zeros of input/output models for control of vortex dynamics," in *American Control Conference*, (Baltimore, MD), IEEE, June 1994.

[4] H.-L. Chang, *Control of Vortex Dynamics*. PhD thesis, UCLA, March 1994.

[5] Eric J. Kostelich and James A. Yorke, "Noise reduction in dynamical systems," *Physical Review A*, vol. 38, pp. 1649–1652, aug 1988.

[6] J.-P. Eckmann, S. Oliffson Kamphorst, D. Ruelle, and S. Ciliberto, "Liapunov exponents from time series," *Physical Review A*, vol. 34, pp. 4971–4979, December 1986.

[7] Alan Wolf, Jack B. Swift, Harry L. Swinney, and John A. Vastano, "Determing lyapunov exponents from a time series," *Physica D*, vol. 16, pp. 285–317, 1985.

[8] Martin Casdagli, "Nonlinear prediction of chaotic time series," *Physica D*, vol. 35, pp. 335–356, 1989.

[9] J. Doyne Farmer and John J. Sidorowich, "Predicting chaotic time series," *Physical Review Letters*, vol. 59, pp. 845–848, aug 1987.

[10] D.S. Broomhead and Gregory P. King, "Extracting qualitative dynamics from experimental data," *Physica D*, vol. 20, pp. 217–236, 1986.

[11] H. Tong, *Non-Linear Time Series*. Oxford Science Publications, New York: Oxford University Press, 1990.

[12] S.-B. Jiang, *Unwindowed Multichannel Lattice Filters and Applications in Adaptive Identification and Control*. PhD thesis, University of California, Los Angeles, 1992.

[13] S.-B. Jiang, J.S. Gibson, A.J. Pearlstein, and A. Glezer, "Adaptive control of a functional differential equation exhibiting some features of the vortex sheet in a plane shear layer," in *Conference on Decision and Control*, (Tucson, Az), IEEE, December 1992.

[14] J.S. Gibson, A. Glezer, and A.J. Pearlstein, "Real-time feedback control of mixing in a plane shear layer," in *AFOSR workshop on turbulence*, (Columbus, OH), April 1991.

[15] P. Tokumaru and P. Dimotakis, "Rotary oscillation control of a cylinder wake," *J. Fluid Mech.*, vol. 224, pp. 77–90, 1991.

[16] K. Roussopoulos, "Feedback control of vortex shedding at low reynolds numbers," *J. Fluid Mech.*, vol. 248, pp. 267–296, 1993.

[17] M. Koochesfahani and P. Dimotakis, "A cancellation experiment in a forced turbulent shear layer," in *First National Fluid Dynamics Congress*, (Cincinnati, Ohio), July 1988. AIAA Paper No.88-3713-CP .

[18] A. Ongoren and D. Rockwell, "Flow structure from an oscillating cylinder, Part 1. Mechanisms of phase shift and recovery in the near wake," *J. Fluid Mech.*, vol. 191, pp. 197–223, 1988.

[19] A. Ongoren and D. Rockwell, "Flow structure from an oscillating cylinder, Part 2. Mode competition in the near wake," *J. Fluid Mech.*, vol. 191, pp. 225–245, 1988.

[20] R. Gopalkrishnan, M. Triantafyllou, G. Triantafyllou, and D. Barrett, "Active vorticity control in a shear flow using a flapping foil," *J. Fluid Mech.*, vol. 274, pp. 1–21, 1994.

[21] V. Rossow, "Lift enhancement by an external trapped vortex," in *10th Fluid and Plasmadynamics Conference*, (Albuquerque, New Mexico), AIAA Paper No. 77-672, June 27–29 1977.

[22] J. Slomski and R. Coleman, "Numerical simulation of vortex generation and capture above an airfoil," in *31st Aerospace Sciences Meeting and Exhibit*, (Reno, Nevada), January 1993. AIAA Paper No. 93-864.

[23] N.-Z. Cao and N. Aubry, "Numerical simulation of a wake flow via a reduced system," *ASME Separated Flows*, vol. FED 149, 1993.

[24] M. Rajaee, S. Karlsson, and L. Sirovich, "Low-dimensional description of free-shear-flow coherent structures and their dynamical behavior," *J. Fluid Mech.*, vol. 258, pp. 1–29, 1994.

[25] L. Cortelezzi, A. Leonard, and J. Doyle, "An example of active circulation control of the unsteady separated flow past a semi-infinite plate," *J. Fluid Mech.*, vol. 260, pp. 127–154, 1994.

[26] C. Brown and W. Michael, "Effect of leading-edge separation on the lift of a delta wing," *J. Aero. Sci.*, vol. 21, pp. 690–694, 1954.

APPENDIX

[1] L. Cortelezzi, "On the Active Control of the Wake Past a Plate with a Suction Point on the Downstream Wall."

[2] C.R. Anderson, H.-L. Chang, and J.S. Gibson, "Adaptive Control of Vortex Dynamics," IEEE Conference on Decision and Control, San Antonio, TX, December 1993.

[3] C.R. Anderson, H.-L. Chang, and J.S. Gibson, "Zeros of Input/Output Models for Control of Vortex Dynamics," American Control Conference, Baltimore, MD, June 1994.

To be submitted for publication to: *Journal of Fluid Mechanics.*

On the active control of the wake past a plate with a suction point on the downstream wall.

by L. CORTELEZZI*

January 19, 1995

Abstract

Active circulation control of the two-dimensional unsteady separated flow past a plate with a suction point on the downstream wall is considered. The rolling-up of the separated shear-layer is modelled by a pair of point vortices whose time-dependent circulation is predicted by an unsteady Kutta condition. A nonlinear controller able to confine the wake to a single vortex pair of constant circulation is derived in closed-form for any free-stream condition. Dynamical system analysis is used to explore the performance of the controlled system. Finally, the control strategy is applied to three different classes of unsteady flows and the results are discussed.

*Department of Mathematics, University of California, Los Angeles, California 90024-1555, U.S.A. E-mail: crtlz@math.ucla.edu

1 Introduction

Active control of unsteady separated fluid flows is attracting wide interest in both the fluid mechanics and control communities because of the many potential engineering applications. See Gad-el-Hak & Bushnell (1991) for a discussion and references. Drag reduction, lift enhancement, noise and vibration control, mixing improvement, etc. are some of the many problems where active control of flows past bluff bodies finds natural applications.

The problem of actively controlling an unsteady fluid flow is in general nonlinear. Since the control of nonlinear systems is still a subject of research, there is no general framework to obtain a desired controller. However, it is well known that the model chosen to represent the plant is of crucial importance in the derivation of the controller. A very complex and detailed model, the full Navier-Stokes equations for example, might generate an overly complex controller or might make the derivation of the controller impossible. On the other hand, an over-simplified or linear model facilitates the derivation of the controller but might generate a controller unable to achieve the desired control objective. A reasonable compromise is a reduced model able to capture the dynamic features of the flow that one wants to control. See Cao and Aubry 1993, Rajaee *et al.* 1994, Cortelezzi *et al.* 1994. Typically, the reduced model is a low-dimensional system governed by a set of ordinary differential equations, while the real flow has infinite dimensions. An advantage of working with a reduced model is that one can use dynamical system analysis to investigate the problem. Analysis of the phase space of the reduced system should provide information about fixed points, limit cycles, bifurcation points, etc., characteristic of the flow under consideration and consequently should provide information about effectiveness and robustness of the controller. Another advantage of model reduction is the potential for producing fast numerical algorithms which are essential for controlling a real flow.

Before attempting to control a laboratory flow one should take the intermediate step of controlling the same class of flows simulated by a more sophisticated CFD (Computational Fluid Dynamics)

code. The application of the controller derived for the reduced model to a complex model should be successful if the two models are dynamically equivalent; i.e., if the phase spaces of the two models are topologically equivalent. The equivalence of the two models can be investigated via dynamical system and time series analysis. There are many advantages in controlling a flow simulated by another CFD code. All the flow quantities necessary to feedback to the controller can be easily measured. The action of the controller is automatically synchronized with the evolution of the flow because both algorithms run in virtual time. Furthermore, the controller can be tested on gradually more complex flows. For example, if the controller were derived for an inviscid model, then it could be applied to the same flow when the fluid is slightly viscous. In general the controller has to be made robust with respect to the perturbations introduced by the new environment, e.g., viscosity, three-dimensionality, background noise (see Doyle *et al.* 1992, Fan *et al.* 1991). Only an iteration process might produce a controller able to handle the flow simulated by the Navier-Stokes equations. Finally, the control of a laboratory flow can be attempted when the controller generated by this chain of refinements is robust enough to perform in the presence of the unmodeled and unpredictable uncertainties affecting the real system and is fast enough to control the flow in real-time.

Recently, efforts to modify certain features of the wake behind bluff and slender bodies, such as reduction or magnification of the wake thickness (Tokumaru & Dimotakis 1991), wake stabilization (Roussopoulos 1993), vortex cancelation (Koochesfahani & Dimotakis 1988), pattern reproduction (Ongoren & Rockwell 1988*a*, *b*, Gopalkrishnan *et al.* 1994), and lift enhancement (Rossow 1977, Slomski & Coleman 1993) have been successful. In all these investigations the free-stream velocity was kept constant and quasi-steady results were achieved usually by moving the body or the actuator with a frequency scaled by the shedding frequency. In a more general situation in which the free-stream velocity is time dependent this approach is generally not sufficient to control the flow and a nonlinear control strategy is necessary.

The present study investigates the active control of the wake past a plate perpendicular to an unsteady fluid flow. In Section 2, following our previous work (see Cortelezzi 1995), we model the unsteady separation from the tips of a flat plate by means of a pair of point vortices whose time-dependent circulation is predicted by an unsteady Kutta condition. The problem is further simplified by imposing wake symmetry. The motion of the vortex pair is determined by a non-linear ordinary differential equation first proposed by Brown and Michael in 1954. A suitable vortex shedding mechanism is also introduced to allow the simulation of flows involving multiple vortices. This reduced model is able to capture the main features of the flow and, for example, is quite accurate for power-law starting flows (see Cortelezzi 1995).

In Section 3, we consider as a control actuator a suction point placed on the downstream wall of the plate. The control objective is to confine the wake to a single vortex pair of constant circulation. We show that suction is a very efficient means to control the production of circulation. Thanks to the simplicity of the model we obtain for any time-dependent free-stream velocity the analytical closed-form solution of the controller; i.e., the predicted suction necessary to inhibit the production of circulation when a vortex pair is present in the flow.

In Section 4, we perform a dynamical system type of analysis to characterize the performance of the controller. When the free-stream is constant, we show the existence of fixed points for the unperturbed system and compute the locus of the fixed points. There is a critical value for the circulation associated with the vortex pair above which one can find two pairs of fixed points: a pair of stable nodes and a pair of saddle points farther downstream. The circulation plays the role of a bifurcation parameter and the vector field undergoes a saddle-node bifurcation when the circulation is near its critical value. The analysis of the phase space shows the existence of a controllable region between the plate and the stable manifolds of the saddle points. When the free-stream velocity oscillates periodically about a unit mean, we compute the Poincaré section to characterized the perturbed system. We show the topological equivalence between the Poincaré section and the phase

space of the unperturbed system. The stable node of the Poincaré section represents a limit cycle while the saddle point represents an unsteady periodic orbit.

In Section 5, we present the results of three simulations. The first two simulations document the ability of the controller to drive the vortex pair to the stable nodes when the free-stream velocity is constant or to a limit cycle when the free-stream velocity oscillates periodically. The third simulation documents the performance of the controller when the free-stream velocity performs pseudo-random oscillations.

2 Mathematical formulation

In this section we introduce a mathematical model of the two-dimensional unsteady separation from the tips of a finite plate with a suction point of strength s at the center of the downstream wall. Let us assume that the regions of vorticity that separate from the boundary layer and are convected away are thin enough to justify a description by means of a vortex sheet. The consequent stretching and rolling up of the vortex sheet, due to the unsteadiness of the flow, suggests a more coarse description via point vortices. The vortex sheet is not completely lost. It is assumed of negligible circulation that connects the feeding point to a point vortex of variable strength which is able to satisfy an unsteady Kutta condition. Mathematically the feeding vortex sheet is just the branch cut due to the logarithmic singularity representing the vortex. All the other vortices in the wake are represented by point vortices of fixed circulation.

We choose, for simplicity, a frame of reference fixed to the plate so that the body can be identified with the segment $[-2ia, 2ia]$ and the suction point s coincides with the point $(0^+, 0)$. Then, the flow of an incompressible irrotational fluid about such a body can be solved via conformal mapping. Using the Joukowski transformation:

$$z = \zeta - \frac{a^2}{\zeta}, \tag{1}$$

we map a finite plate of length $L = 4a$ in the z-plane onto the circle of radius a in the ζ-plane (see Figure 1) preserving the characteristic of the flow at infinity.

To make the problem dimensionless we have to define a characteristic length and time scale. For this purpose we write the free-stream velocity as follows:

$$U(t) = U_\infty + u(t), \tag{2}$$

where U_∞ is the unperturbed free-stream velocity and $u(t)$ is the time dependent component. If we choose the circle radius as characteristic length and a/U_∞ as characteristic time of the problem then we can define the following dimensionless quantities:

$$\begin{aligned} z^* &= \frac{z}{a}, \qquad \zeta^* = \frac{\zeta}{a}, \qquad a^* = 1, \qquad t^* = \frac{U_\infty t}{a}, \\ U^* &= \frac{U}{U_\infty} = 1 + \epsilon_U, \qquad \Gamma^* = \frac{\Gamma}{U_\infty a}, \qquad s^* = \frac{s}{U_\infty a}. \end{aligned} \tag{3}$$

where Γ is the circulation. Note that $\epsilon_U = u/U_\infty$ contains the unsteadiness of the free-stream velocity and it is not necessarily small with respect to unit. We now continue the mathematical formulation of the problem using dimensionless variables, the stars will be dropped for convenience.

There is experimental evidence (Lisosky 1993, private communication) that the near wake is nearly two dimensional and symmetric about the x-axis if the plate moves with a non-zero acceleration. Under these circumstances the problem can be simplified imposing symmetry with respect to the real axis, i.e., the vortices have equal and opposite circulation, Γ_n and $-\Gamma_n$, and are located in complex conjugate positions, ζ_n and $\bar{\zeta_n}$, respectively. Since the velocity field has to satisfy Laplace's equation and the boundary condition in the mapped plane can be treated using the circle theorem, we can build the complex potential F superimposing basic flows. Thus, the complex velocity field $w = dF/d\zeta$ has the form:

$$\begin{aligned} w(\zeta,t) = U\left(1 - \frac{1}{\zeta^2}\right) &+ \frac{i\Gamma_1}{2\pi}\left(\frac{1}{\zeta - \zeta_1} + \frac{\bar{\zeta_1}}{1 - \zeta\bar{\zeta_1}} - \frac{1}{\zeta - \bar{\zeta_1}} - \frac{\zeta_1}{1 - \zeta\zeta_1}\right) \\ &+ \sum_{n=2}^{N} \frac{i\Gamma_n}{2\pi}\left(\frac{1}{\zeta - \zeta_n} + \frac{\bar{\zeta_n}}{1 - \zeta\bar{\zeta_n}} - \frac{1}{\zeta - \bar{\zeta_n}} - \frac{\zeta_n}{1 - \zeta\zeta_n}\right) - s\frac{\zeta + 1}{\zeta(\zeta - 1)}. \end{aligned} \tag{4}$$

Note that for convenience we are departing from the usual convention and taking the circulation positive when in the clockwise sense. Note also that the singularity on the back face of the plate behaves as a sink when $s > 0$ and as a source otherwise. We impose the Kutta condition to regularize the potential flow at the tips of the plate. In the ζ-plane the flow is non-singular since the singularity has been absorbed by the mapping. To remove the singularity in the z-plane the complex velocity (4) in the mapped plane has to be zero at the top and bottom of the circle, i.e., at $\zeta = \pm i$. Solving for Γ_1 we obtain:

$$\Gamma_1 = -\pi i \frac{(1+\zeta_1^2)(1+\bar{\zeta}_1^2)}{(\zeta_1-\bar{\zeta}_1)(1-\zeta_1\bar{\zeta}_1)} \left[2U - \sum_{n=2}^{N} \frac{i\Gamma_n}{\pi} \frac{(\zeta_n-\bar{\zeta}_n)(1-\zeta_n\bar{\zeta}_n)}{(1+\zeta_n^2)(1+\bar{\zeta}_n^2)} + s \right]. \tag{5}$$

Note that the circulation associated with the vortex pair depends on all the flow quantities, i.e., free-stream velocity U, suction s, position and circulation of all the vortex pairs, and the position of the vortex pair 1. The above expression suggests that the Kutta condition can be satisfied even when there are no vortices in the flow. It suffice to choose $s(t) = -2U(t)$, see Figure 2.

To describe the motion of the vortex pair in the physical plane we use the following set of ordinary differential equations:

$$\begin{cases} \dfrac{d\bar{z}_1}{dt} + (\bar{z}_1 + 2i)\dfrac{1}{\Gamma_1}\dfrac{d\Gamma_1}{dt} = \lim\limits_{z\to z_1} \left\{ \dfrac{d}{dz}\left[F - \dfrac{i\Gamma_1}{2\pi}\log(z-z_1) \right] \right\} \\ \dfrac{d\bar{z}_r}{dt} = \lim\limits_{z\to z_r} \left\{ \dfrac{d}{dz}\left[F - \dfrac{i\Gamma_r}{2\pi}\log(z-z_r) \right] \right\}, \end{cases} \tag{6}$$

with the initial conditions:

$$\begin{cases} z_1(t_s) = 2i \\ z_r(t_s) = z_{r_s} \qquad r = 2...N. \end{cases} \tag{7}$$

The term containing $d\Gamma_1/dt$ is known as Brown and Michael's correction (Brown and Michael 1954). The motion of the vortex of variable strength described by this equation guarantees no net force on the vortex and its connecting cut. The limit on the right hand side, which represents the complex

velocity at the vortex location without the self-induced contribution, produces the so called Routh's correction when it is evaluated in the mapped plane (e.g. Clements 1973).

We solve the problem in the mapped plane. Once we have performed the change of variables, substituted for the complex potential, and carried out the limit required in the equation (6), we obtain:

$$
\begin{cases}
\left[\dfrac{\bar{\zeta}_1^2+1}{\bar{\zeta}_1^2}+\dfrac{(\bar{\zeta}_1+i)^2}{\bar{\zeta}_1}\dfrac{(1+\zeta_1^2)(1-\bar{\zeta}_1^2)}{(1+\bar{\zeta}_1^2)(\zeta_1-\bar{\zeta}_1)(1-\zeta_1\bar{\zeta}_1)}\right]\dfrac{d\bar{\zeta}_1}{dt} \\
\qquad -\left[\dfrac{(\bar{\zeta}_1+i)^2}{\bar{\zeta}_1}\dfrac{(1-\zeta_1^2)(1+\bar{\zeta}_1^2)}{(1+\zeta_1^2)(\zeta_1-\bar{\zeta}_1)(1-\zeta_1\bar{\zeta}_1)}\right]\dfrac{d\zeta_1}{dt}= \\
\left(\dfrac{\zeta_1^2}{1+\zeta_1^2}\right)\left\{U\left(1-\dfrac{1}{\zeta_1^2}\right)+\dfrac{i\Gamma_1}{2\pi}\left[\dfrac{\bar{\zeta}_1}{1-\zeta_1\bar{\zeta}_1}-\dfrac{1}{\zeta_1-\bar{\zeta}_1}-\dfrac{\zeta_1}{1-\zeta_1^2}\right]+\dfrac{i\Gamma_1}{2\pi}\dfrac{1}{\zeta_1(1+\zeta_1^2)}\right. \\
\left.+\sum_{n=2}^{N}\dfrac{i\Gamma_n}{2\pi}\dfrac{(1-\zeta_1^2)(\zeta_n-\bar{\zeta}_n)(1-\zeta_n\bar{\zeta}_n)}{(\zeta_1-\zeta_n)(\zeta_1-\bar{\zeta}_n)(1-\zeta_1\zeta_n)(1-\zeta_1\bar{\zeta}_n)}-s\dfrac{\zeta_1+1}{\zeta_1(\zeta_1-1)}\right\} \\
-\dfrac{(\bar{\zeta}_1+i)^2}{\bar{\zeta}_1}\left[2\dfrac{dU}{dt}-\sum_{n=2}^{N}\dfrac{i\Gamma_n}{\pi}\left[\dfrac{1-\zeta_n^2}{(1+\zeta_n^2)^2}\dfrac{d\zeta_n}{dt}-\dfrac{1-\bar{\zeta}_n^2}{(1+\bar{\zeta}_n^2)^2}\dfrac{d\bar{\zeta}_n}{dt}\right]+\dfrac{ds}{dt}\right] \\
\qquad \left[2U-\sum_{n=2}^{N}\dfrac{i\Gamma_n}{\pi}\dfrac{(\zeta_n-\bar{\zeta}_n)(1-\zeta_n\bar{\zeta}_n)}{(1+\zeta_n^2)(1+\bar{\zeta}_n^2)}+s\right]^{-1} \\
\dfrac{d\bar{\zeta}_r}{dt}=\left[\dfrac{\zeta_r^2\bar{\zeta}_r^2}{(1+\zeta_r^2)(1+\bar{\zeta}_r^2)}\right]\left\{U\left(1-\dfrac{1}{\zeta_r^2}\right)+\dfrac{i\Gamma_r}{2\pi}\left[\dfrac{\bar{\zeta}_r}{1-\zeta_r\bar{\zeta}_r}-\dfrac{1}{\zeta_r-\bar{\zeta}_r}-\dfrac{\zeta_r}{1-\zeta_r^2}\right]\right. \\
\left.+\dfrac{i\Gamma_r}{2\pi}\dfrac{1}{\zeta_r(1+\zeta_r^2)}+\sum_{n\neq r}^{N}\dfrac{i\Gamma_n}{2\pi}\dfrac{(1-\zeta_r^2)(\zeta_n-\bar{\zeta}_n)(1-\zeta_n\bar{\zeta}_n)}{(\zeta_r-\zeta_n)(\zeta_r-\bar{\zeta}_n)(1-\zeta_r\zeta_n)(1-\zeta_r\bar{\zeta}_n)}-s\dfrac{\zeta_r+1}{\zeta_r(\zeta_r-1)}\right\},
\end{cases}
\tag{8}
$$

with the initial conditions:

$$
\begin{cases}
\zeta_1(t_s)=i \\
\zeta_r(t_s)=\zeta_{r_s} \qquad r=2...N,
\end{cases}
\tag{9}
$$

where Γ_1 is given by (5). Note because of Brown and Michael's correction the equations are coupled not just through the position of the vortices but also through the velocity of the vortices.

The forces acting on the plate are of particular interest because they can be measured experi-

mentally and are the crucial quantities in any problem involving the interaction between fluids and structures. The forces can be computed by means of the Blasius theorem, see Cheers 1979, Graham 1980, and Cortelezzi 1995 for different derivations. The drag has the following form:

$$D = 4\pi\rho\frac{dU}{dt} + 4\pi\rho\frac{ds}{dt} + i\rho\frac{d}{dt}\left[\frac{\Gamma_1(1-\zeta_1\bar{\zeta}_1)(\zeta_1-\bar{\zeta}_1)}{\zeta_1\bar{\zeta}_1}\right] + i\rho\sum_{n=2}^{N}\Gamma_n\frac{d}{dt}\left[\frac{(1-\zeta_n\bar{\zeta}_n)(\zeta_n-\bar{\zeta}_n)}{\zeta_n\bar{\zeta}_n}\right]. \quad (10)$$

The component of the force along the imaginary axis, i.e. the lift, is zero because of the imposed symmetry. The first term on the right hand side is the force due to added mass, i.e., is the inertia of the attached flow, the second term is the contribution due to suction and the last two terms are the contribution due to the evolution of the wake. We define the drag coefficient as follow:

$$C_D = \frac{D}{\frac{1}{2}\rho U_\infty^2 L} \quad (11)$$

Note that the drag coefficient is well defined only in the case where the free-stream velocity is constant. To compute the drag coefficient in the unsteady cases that we will present in Section 5 we choose for U_∞ the asymptotic value or the mean value of the free-stream velocity.

The final element necessary for a correct implementation of this model is a vortex shedding mechanism. If we envision the separation process by means of a vortex sheet then the instantaneous circulation necessary to keep the flow regular at the tip of the plate is associated with an infinitesimal segment of the sheet which is then shed in the fluid. The circulation is consequently distributed along the singular line and the sheet rolls-up around the points of highest absolute circulation per unit length and it stretches most where the circulation per unit length is lowest. As the process continues, we observe that a large amount of circulation concentrates in the core of the spirals which are connected with each other by filaments of almost negligible circulation. This process can be reflected in our model by replacing each spiral with a point vortex of fixed circulation except for the spiral connected to the separation point which is replaced by a point vortex with time-dependent circulation. This latter vortex will continue to be fed circulation until the rate of change of circulation

becomes zero because we conjecture that this is the part of the sheet that will be stretched the most.

Let us consider the problem of shedding a new vortex when $N-1$ other vortices are already present in the flow. If t_s is the shedding time then it is crucial to analyze the transition from t_s^- to t_s^+. Up to the time t_s^- vortex 1 has variable strength such that the Kutta condition is satisfied. At time $t = t_s$ this vortex has its strength frozen and all the vortices renumbered. Finally at t_s^+ a new vortex 1 is introduced into the flow to remove the square root singularity. If we restrict our simulation to the case where the shed vortices have alternate sign, then we can model the vortex shedding making the assumption that the time $t = t_s$ is determined by the condition:

$$\left.\frac{d\Gamma_1}{dt}\right|_{t=t_s} = 0, \tag{12}$$

assuming $d^2\Gamma_1/dt^2\big|_{t=t_s} \neq 0$. Any other choice for the shedding time implies the arbitrary production of two sequential vortices of the same sign or the existence of a vortex which strength decreases in time. The latter situation is physically unacceptable. This procedure has been proposed by Graham (1980) to simulate the flow induced by an oscillating diamond shaped cylinder.

The quality of the simulation with many vortices depends in large part on the shedding mechanism. Let us assume that between two zero crossings $d\Gamma_1/dt$ is positive and has two peaks, then it is not clear whether one or two vortices should be shed during this period. It seems that the deepness of the trough separating the peaks would be an important parameter. If it is very deep it seems reasonable to have two vortices otherwise just one. Although the shedding mechanism can be implemented for all cases, to avoid any ambiguity we restrict ourselves to cases where the rate of circulation production has only one local maximum or minimum between consecutive zero crossings or, equivalently, where $d^2\Gamma_1/dt^2$ does not change sign between crossings.

Because of the size and complexity of the problem we are not attempting an analytical solution. We solve the problem numerically taking advantage of our previous work (Cortelezzi 1995).

3 Active wake control

There are different approaches one can use to control the wake past plate by suction. One can try to control the position of the vortices or some features of the velocity field. We choose to control the amount of circulation injected in the flow because we believe that this is the most efficient way to control the wake. To gain insight on the effectiveness of the suction as a mean to control the circulation we compute the rate of circulation production by taking the time derivative of (5), we have:

$$\frac{d\Gamma_1}{dt} = -\frac{\pi i}{(\zeta_1-\bar{\zeta}_1)(1-\zeta_1\bar{\zeta}_1)}\left[2U - \sum_{n=2}^{N}\frac{i\Gamma_n}{\pi}\frac{(\zeta_n-\bar{\zeta}_n)(1-\zeta_n\bar{\zeta}_n)}{(1+\zeta_n^2)(1+\bar{\zeta}_n^2)} + s\right]$$
$$\left[(1+\bar{\zeta}_1^2)^2(1-\zeta_1^2)\frac{d\zeta_1}{dt} - (1+\zeta_1^2)^2(1-\bar{\zeta}_1^2)\frac{d\bar{\zeta}_1}{dt}\right] \qquad (13)$$
$$-\pi i\frac{(1+\zeta_1^2)(1+\bar{\zeta}_1^2)}{(\zeta_1-\bar{\zeta}_1)(1-\zeta_1\bar{\zeta}_1)}\left[2\frac{dU}{dt} - \sum_{n=2}^{N}\frac{i\Gamma_n}{\pi}\left[\frac{1-\zeta_n^2}{(1+\zeta_n^2)^2}\frac{d\zeta_n}{dt} - \frac{1-\bar{\zeta}_n^2}{(1+\bar{\zeta}_n^2)^2}\frac{d\bar{\zeta}_n}{dt}\right] + \frac{ds}{dt}\right].$$

From the above expression we see that the rate of circulation production depends on all flow quantities and their derivatives. Note that suction and rate of change of suction contribute to the production of circulation in the same way as free-stream velocity and free-stream acceleration, respectively. Hence, using suction as mean to control the rate of circulation production is as powerful and robust as using the free-stream velocity.

Our control objective is to inhibit the rate of circulation production after the starting vortex pair is shed in the flow. In other words, we want to predict the suction so that once the starting vortex pair is shed in the flow the Kutta condition remains satisfied without requiring a new vortex pair. The possibility to maintain the wake confined to a controlled recirculating bubble has important implication to the problem of drag reduction in general, moreover, it can provide insight into vortex management techniques for the three-dimensional flow over a delta wing, see Rao 1987. Note that there is no conceptual difficulty in inhibiting the rate of circulation production when more than a vortex pair in present in the wake, if that is required by the application under consideration.

Let t_s be the time when the starting vortex pair is shed in the flow, i.e. the time when the rate of circulation production goes to zero. Then for $0 \leq t \leq t_s$ the motion of the vortex pair of time-dependent circulation is prescribed by the following equation:

$$\left[\frac{\bar{\zeta}_1^2+1}{\bar{\zeta}_1^2}+\frac{(\bar{\zeta}_1+i)^2}{\bar{\zeta}_1}\frac{(1+\zeta_1^2)(1-\bar{\zeta}_1^2)}{(1+\bar{\zeta}_1^2)(\zeta_1-\bar{\zeta}_1)(1-\zeta_1\bar{\zeta}_1)}\right]\frac{d\bar{\zeta}_1}{dt}-\left[\frac{(\bar{\zeta}_1+i)^2}{\bar{\zeta}_1}\frac{(1-\zeta_1^2)(1+\bar{\zeta}_1^2)}{(1+\zeta_1^2)(\zeta_1-\bar{\zeta}_1)(1-\zeta_1\bar{\zeta}_1)}\right]\frac{d\zeta_1}{dt}=$$

$$\left(\frac{\zeta_1^2}{1+\zeta_1^2}\right)\left\{U\left(1-\frac{1}{\zeta_1^2}\right)+\frac{i\Gamma_1}{2\pi}\left[\frac{\bar{\zeta}_1}{1-\zeta_1\bar{\zeta}_1}-\frac{1}{\zeta_1-\bar{\zeta}_1}-\frac{\zeta_1}{1-\zeta_1^2}\right]+\frac{i\Gamma_1}{2\pi}\frac{1}{\zeta_1(1+\zeta_1^2)}-s\frac{\zeta_1+1}{\zeta_1(\zeta_1-1)}\right\}$$

$$-\frac{(\bar{\zeta}_1+i)^2}{\bar{\zeta}_1}\left[2\frac{dU}{dt}+\frac{ds}{dt}\right][2U+s]^{-1} \tag{14}$$

with the initial condition:

$$\zeta_1(0)=i. \tag{15}$$

Note that suction appears in the above equation but in this study it is not used to control the flow for $t \leq t_s$. In general, suction can be used to drive the system to some desired state from which, at $t = t_s$, the controller that inhibits the production of circulation takes over.

When, instead, $t \geq t_s$ the equation of motion for the vortex pair of constant circulation $\pm\Gamma_{1_s}$ is:

$$\frac{d\bar{\zeta}_1}{dt}=\left[\frac{\zeta_1^2\bar{\zeta}_1^2}{(1+\zeta_1^2)(1+\bar{\zeta}_1^2)}\right]\left\{U\left(1-\frac{1}{\zeta_1^2}\right)+\frac{i\Gamma_{1_s}}{2\pi}\left[\frac{\bar{\zeta}_1}{1-\zeta_1\bar{\zeta}_1}-\frac{1}{\zeta_1-\bar{\zeta}_1}-\frac{\zeta_1}{1-\zeta_1^2}\right]\right.$$

$$\left.+\frac{i\Gamma_{1_s}}{2\pi}\frac{1}{\zeta_1(1+\zeta_1^2)}-s\frac{\zeta_1+1}{\zeta_1(\zeta_1-1)}\right\}, \tag{16}$$

with the initial condition:

$$\zeta_1(t_s)=\zeta_{1_s}. \tag{17}$$

To close the problem we have to provide an equation for s which implements our control strategy. An ordinary differential equation for s can be obtained from (13) simply setting $d\Gamma_1/dt = 0$ and $\Gamma_n = 0$, for $n = 2, 3, ..., N$. Nevertheless, a simpler result follows from the fact that the problem of maintaining $d\Gamma_1/dt = 0 \quad \forall t > t_s$, is equivalent to the problem of maintaining the Kutta condition satisfied when a vortex pair of fixed circulation is present in the flow. Then the suction which

implements our control strategy is simply derived by solving (5) for s when $\Gamma_n = 0$, $n = 2, 3, ..., N$. We have:

$$s = -2U - \pi i \Gamma_1 \frac{(\zeta_1 - \bar{\zeta}_1)(1 - \zeta_1 \bar{\zeta}_1)}{(1 + \zeta_1^2)(1 + \bar{\zeta}_1^2)}. \tag{18}$$

A question arises about the compatibility of the equations (14) and (16). Compatibility is required to guarantee a smooth transition, at time $t = t_s$, from the final state of equation (14) to the initial state of equation (16). At time $t = t_s$ the Brown and Michael correction vanishes and the two equation coincide, consequently compatibility is assured.

4 Dynamical behavior of the controlled system

In the previous section we have been able to find a controller which inhibits the production of circulation when a vortex pair is present in the flow. This section is devoted to the analysis of the dynamical behavior of the controlled system.

As initial step we search for the fixed points of the unperturbed system. For convenience we rewrite equation (16) in polar form, see Figure 1. We obtain:

$$\begin{cases} \dfrac{d\rho_1}{dt} = \dfrac{\rho_1}{\rho_1^4 + 1 - 2\rho_1^2 \cos 2\theta_1} \left[U\rho_1(\rho_1^2 - 1)\sin\theta_1 - \dfrac{s\rho_1^2(\rho_1^2 - 1)}{\rho_1 + 1 - 2\rho_1 \sin\theta_1} \right. \\ \qquad\qquad \left. + \dfrac{\Gamma_1 \rho_1^2 [8\rho_1^2(\rho_1^4 + 1 - 2\rho_1^2 \sin\theta_1)\cos^2\theta_1 - (\rho_1^4 - 1)^2]\sin\theta_1}{4\pi[(\rho_1^4 + 1)^2 - 4\rho_1^2 \cos^2 2\theta_1]\cos\theta_1} \right] \\ \dfrac{d\theta_1}{dt} = \dfrac{\rho_1}{\rho_1^4 + 1 - 2\rho_1^2 \cos 2\theta_1} \left[U(\rho_1^2 + 1)\cos\theta_1 + \dfrac{2s\rho_1^2 \cos\theta_1}{\rho_1 + 1 - 2\rho_1 \sin\theta_1} \right. \\ \qquad\qquad \left. + \dfrac{\Gamma_1 \rho_1 (\rho_1^2 + 1)[8\rho_1^2(\rho_1^4 + 1 - 2\rho_1^2 \cos\theta_1)\cos^2\theta_1 + (\rho_1^2 - 1)^4]}{4\pi(\rho_1^2 - 1)[(\rho_1^4 + 1)^2 - 4\rho_1^2 \cos^2 2\theta_1]} \right] \end{cases} \tag{19}$$

where

$$s = \frac{\Gamma_1}{\pi} \frac{2\rho_1(\rho_1^2 - 1)\cos\theta_1}{\rho_1^4 + 1 - 2\rho_1^2 \cos 2\theta_1} - 2U. \tag{20}$$

With the term unperturbed system we intend the case where all the flow quantities are constant. Note that in the above equations the free-stream velocity is indicated with U for clarity although it

is simply unit. Consequently, the problem depend only on one the parameter: the circulation of the vortex, Γ_1.

When suction is zero there does not exist any vortex pair which is stationary and satisfy the Kutta condition beside the pathological situations where the vortex pair has infinite circulation and is infinitely distant from the plate. This result predicts that for any free-stream velocity a flow which separates from the tips of a flat plate cannot reach a steady-state solution. At the best of our knowledge there is not any experimental evidence which contradicts this prediction. When, instead, suction is non-zero there are fixed points and the locus of them is shown in Figure 4. Each point on this curve represents the position of a vortex, whose circulation is shown in Figure 5(b), that is stationary and satisfies the Kutta condition. The suction associated with each fixed point is shown in Figure 5(a). The reader should be aware that because of symmetry we will restrict our discussion to the upper half of the domain.

We conduct a linear stability analysis to investigate the nature of the fixed points. Figure 3 shows real and imaginary parts of the eigenvalues λ_1 and λ_2. Three distinct regions can be recognized. Near the plate, where $0 < x < x_1$, the eigenvalues λ_1 and λ_2 are complex conjugate with positive real parts, see Figure 3. In this region the fixed points are unstable foci. Figure 5 shows that both, circulation and suction, are negative. Physically it means that the Kutta condition is unusually satisfied by a vortex generating a counterclockwise flow and by injecting fluid. In particular, when $x = 0$, there are no vortices in the flow and the case shown in Figure 2 is recovered. In the middle region, where $x_1 < x < x_2$, the eigenvalues are purely real with $\lambda_1 < \lambda_2 < 0$, see Figure 3. In this region the fixed points are stable nodes. Circulation and suction are both positive as expected, see Figure 5. Note that the values of circulation and of suction at $x = x_2^-$ are the minimum values necessary to have a stable fixed point, $\Gamma_c \approx 18.49$ and $s_c \approx 0.67$ respectively. Note also that the asymptote at $x = x_1$ separates two regions of totally different dynamics and no smooth transition is possible between the two regions as both, circulation and suction, are discontinuous passing through

x_1. In the third region, where $x > x_2$, the eigenvalues are purely real with $\lambda_1 < 0 < \lambda_2$, see Figure 3. In this region the fixed points are saddle points. As before, circulation and suction are both positive, see Figure 5. The circulation increases from Γ_c to infinite while the suction decreases monotonically to zero as x goes from x_2 to infinite. Note that at $x = x_2$ the eigenvalue λ_2 becomes zero providing a necessary but not sufficient condition for the bifurcation of a fixed point.

We restrict our discussion to the sub-domain where $x > x_1$, $\Gamma_{1_v} > 0$, and $s > 0$. It is important to observe that in this sub-domain there are fixed points only when $\Gamma_{1_v} \geq \Gamma_c$. As suggested by the behavior of the eigenvalue λ_2 the vector field undergoes to a saddle-node bifurcation at $x = x_2$ when $\Gamma_{1_v} = \Gamma_c$. The circulation of the vortex, Γ_{1_v}, plays hence the role of bifurcation parameter. Technically, the bifurcation should be analyzed using the center manifold theorem (see Guckenheimer and Holmes, Chp.4), but to maintain the paper focused on fluid-mechanics we will skip this formal step. To document the effect of the bifurcation parameter and to give a complete characterization of the dynamics of the system we plot the sub-space of the phase space which coincides with the physical domain. In this plane the lines of flow of the vector field coincide with the trajectories of the vortex. The reader should be aware that these trajectories are obtained for constant free-stream velocity and circulation while suction in general changes along each trajectory. When $\Gamma_{1_v} < \Gamma_c$ there are no fixed points. There are only two families of trajectories separated by the center manifold, see Figure 6(a). When a vortex starts above the center manifold it drifts irreversibly downstream. When, instead, the vortex starts below the center manifold it can, depending on its initial position, approach temporarily the plate, but eventually drifts downstream. When $\Gamma_{1_v} = \Gamma_c$ there is a non-hyperbolic fixed point and the flow pattern of the center manifold can be easily recognized, see Figure 6(b). Finally, when $\Gamma_{1_v} > \Gamma_c$ there are two hyperbolic fixed points: a stable node and a saddle point, see Figure 6(c). The vortex trajectory is characterized by the initial position of the vortex with respect to the stable manifold of the saddle point. If the vortex is initially on the left of the stable manifold then is driven by the controller to the stable node. It is interesting to observe

that the trajectories between the stable manifold and the x-axis extend infinitely downstream. When the vortex and its image are initially in the narrow region delimited by the stable manifold and the image manifold, they propel themselves upstream and, with the help of suction, first approach the plate and then are driven to the stable node and its image. When, instead, the vortex is initially on the right of the stable manifold it drifts downstream even if temporarily approaches the plate. We define as controllability region the basin of attraction of the stable node, i.e., the region delimited by the coordinate axes and the stable manifold of the saddle point. Note that as Γ_1, increases the distance between stable node and saddle point increases as well, with a consequent widening of the controllability region.

Since our final goal is to control the wake past the plate in the presence of an unsteady free-stream condition, it is crucial to investigate how the phase space modifies under a time-dependent perturbation. The answer to this question is given by a theorem (see Guckenheimer and Holmes, Chp. 4) which guarantees that the Poincaré section of a periodically perturbed system is topologically equivalent, for sufficiently small perturbations, to the phase space of the unperturbed system provided that the fixed points are hyperbolic. We perturb our system with a free-stream velocity of the form $U(t) = 1 + \epsilon \sin(\omega t)$ and compute the Poincaré section by plotting the vortex position at $t = 2n\pi/\omega$ for $n = 0, 1, 2, \ldots$. The resulting Poincaré section presents two hyperbolic fixed points: a stable node and a saddle point, see Figure 6(d). The stable node represents a limit cycle and the saddle point an unstable periodic orbit. As we should show in the next section, see Figure 13, the vortex is driven to a periodic orbit if it is initially on the left of the stable manifold of the Poincaré section. The topological equivalence between the phase space and the Poincaré section becomes evident comparing Figures 6(c) and 6(d). Because of this equivalence we can extend the definition of controllability region to the perturbed system. The controllability region coincides with the basin of attraction of the stable node of the Poincaré section.

In conclusion, suction is a robust mean to control the wake past a plate both in perturbed and

unperturbed conditions provided that the vortex is initially within the controllability region. In the unperturbed case the vortex is driven to the stable node while in the periodically perturbed case is driven on a periodic orbit.

5 Results

In this section we present the results of three simulations. The first two simulations document the ability of the controller of driving the vortex to the stable node when the free-stream velocity is constant or to a limit cycle when the free-stream velocity oscillates periodically. The third simulation documents the performance of the controller when the free-stream velocity performs pseudo-random oscillations.

In the first simulation the free-stream velocity increases from rest, reaches a maximum value, and decreases to a unit value at $t = 1$, see Figure 7. We carefully choose the initial evolution of the free-stream velocity so that, in all three simulations, a vortex pair of nearly the same circulation $\Gamma_{1_s} > \Gamma_c$ is shed in the flow at nearly the same time. For simplicity suction is used to control the wake only after the rate of circulation production is gone to zero, see Figures 7 and 9. Three distinct intervals of time can be recognized. Initially, when $0 < t < t_s$, the flow is uncontrolled and separates from the tips of the plate creating a vortex pair which drifts downstream, Figure 8 shows the trajectory of the top vortex. The the rate of circulation production associated with the top vortex increases initially, decreases during the deceleration, and eventually become zero at $t = t_s \approx 0.71$ triggering the controller, see Figure 9. At the same time the circulation of the top vortex reaches its maximum and final value, see Figure 9. The drag is dominated by the effect of the added mass because of the strong accelerations of the flow, see Figure 10. In the second interval, $t_s < t < 1$, the controller predicts the suction necessary to maintain the wake to a single vortex pair of constant circulation, $\Gamma_{1_s} = \pm 20.01$, see Figures 7 and 9. The flow is still decelerating and the suction increases rapidly driving the vortices away from their drifting trajectories and toward the

x-axis, see Figures 7 and 8. The drag increases suddenly because of the effect of suction, but quickly decreases and becomes negative as the effect of the added mass returns to dominate, see Figure 10. Finally, when $t > 1$, free-stream velocity and circulation are constants and suction drives the vortex pair to the stable node. Note that the vortex pair moves on the trajectory predicted by the analysis in Section 4, see for a comparison Figures 6(c) and 8. The drag increases from its minimum value and eventually reaches a zero value as the added mass effect subdues, see Figure 10. Figures 11(a)-(f) show the instantaneous streamlines during the capturing process, because of symmetry we plot only the top half of the domain. Figure 11(a) and (b) show the flow at time $t < t_s$, where two recirculating bubbles grow and merge together. As suction becomes non-zero the recirculating bubble is newly splitted in two bubbles, see Figure 11(c). Figures 11(c)-(f) show how the vortex is driven to the fixed point. Figures 11(e)-(f) are nearly identical because the flow has almost reached its steady state.

In the second simulation the free-stream velocity increases from rest and reaches a maximum value, as in the first simulation, but then oscillates about unit mean value, see Figure 12. Note that the amplitude of the oscillations is such that the flow reverses its direction for nearly one third of the period of oscillation creating one of the worse possible scenario for the controller. Three distinct intervals of time can be recognized. Initially, when $0 < t < t_s$, the flow behaves qualitatively as in the first simulation, see Figures 12-15. The rate of circulation production becomes zero at $t = t_s \approx 0.70$. In the second interval, $t_s < t < 2$, the controller predicts the suction necessary to maintain the wake to a single vortex pair of constant circulation, $\Gamma_{1_s} \approx \pm 20.15$, see Figures 7 and 9. Suction increases at first, then after a fluctuation it reaches its maximum absolute value, and finally suction decreases sharply. As a result the vortices are driven away from their drifting trajectories, at first toward the origin and then toward the tip of the plate. At the end of the first period the vortices are positioned near to the limit cycle trajectories, see Figure 13. The drag increases suddenly because of the effect of suction, then decreases because of the added mass effect, and finally presents a sharp peak because

of the combined effects of flow acceleration and suction fluctuation, see Figure 15. Finally, when $t > 2$, all the flow quantities reach rapidly their final periodic behavior while the circulation of the vortex pair is maintained constant, see Figures 12-15. The vortices are rapidly driven on the limit cycle trajectories where they orbit for the rest of the simulation, see Figure 13. Figures 16(a)-(l) show the instantaneous streamlines during one period of oscillation, $6 < t < 8$, as the vortices move clockwise on the limit cycle trajectories.

In the final simulation the free-stream velocity increases from rest and reaches a maximum value, as in the previous simulations, but then performs pseudo-random oscillations about unit mean value, see Figure 17. Initially, when $0 < t < t_s$, the flow behaves qualitatively as in the previous simulations, see Figures 17-20. At time $t = t_s \approx 0.70$ the rate of circulation production goes to zero triggering the controller which maintains the wake, for the rest of the simulation to a single vortex pair of constant circulation, $\Gamma_{1_s} \approx \pm 20.15$, see Figures 17 and 19. Because of the pseudo-random character of the the free-stream velocity it is difficult to give an interpretation to the time evolution of suction in term of the evolution of the flow. We can only say that suction is able to maintain the vortices closed to the plate orbitating on rather complex trajectories. Note that the trajectories somehow entangles around the position of the stable nodes of the unperturbed system, see Figures 6(c) and 18.

6 Conclusions

A point vortex model has been used to simulate the unsteady separated flow past a flat plate with a suction point on the downstream wall. For this model we derived a control strategy that confines the wake to a single vortex pair of constant circulation. Because of the simplicity of the model we obtained the analytical closed-form solution of the nonlinear controller for any free-stream velocity. The performance of the controller was characterized by a dynamical system type of analysis. In the case of steady flow we computed the locus of the fixed points of the unperturbed system. We

showed that a pair of stable nodes and a pair of saddle points exist only if the circulation associated with the vortex pair is above a critical value. We also showed that the vector field presents a saddle-node bifurcation and that the circulation is the bifurcation parameter. We identified the controllable region of the unperturbed system with the basins of attraction of the nodes. In the case of unsteady flow we computed the Poincaré section of the perturbed system. We presented evidence of the topological equivalence between phase space of the unperturbed system and Poincaré section. We showed that under perturbation the stable nodes of the unperturbed system become periodic orbits. We identified the controllable region of the perturbed system as the basin of attraction of the nodes of the Poincaré section. The predictions of our analysis were verified by testing the controller with three different unsteady free-stream conditions. The first simulation documented the ability of the controller of driving the vortex pair to the stable nodes when the free-stream is asymptotically constant. The second simulation documented the ability of the controller of driving the vortex pair to the periodic orbits when the free-stream velocity oscillates periodically about a unit mean. Finally, the third simulation showed the successful performance of the controller when the free-stream velocity performs pseudo-random oscillations about a unit mean.

The present study showed that the use of a reduced model provides a favorable environment to derive the desired control strategy and to test its performance and robustness. The natural continuation of the present work would be embedding the derived controller into a more complex and realistic model, for example, the Navier-Stokes equations. The embedding process should be supported by a dynamical system and time series analysis to demonstrate the dynamical equivalence of the two models. Testing the controller in a different numerical environment instead of in an experiment presents several advantages. All the flow quantities necessary to feedback to the controller can be easily measured. The action of the controller is automatically synchronized with the evolution of the flow. Finally, the controller can be easily tested on gradually more complex flows allowing the researcher to make the controller progressively robust with respect to different types of perturba-

tions (e.g. viscosity, three-dimensionality, back-ground noise, etc.). Successful completition of this process would open the possibilities for the active control of large-scale coherent vortical structures in engineering applications.

7 Acknowledgments

The author wishes to thank Dr. F.E. Marble for suggesting the use of a suction point as a means to control the flow. The author also wishes to thank Dr. R. Camassa and Dr. J.S. Gibson for several valuable discussions. This work was supported by the Air Force Office for Scientific Research Grant # F49620-92-J-0279.

Figures

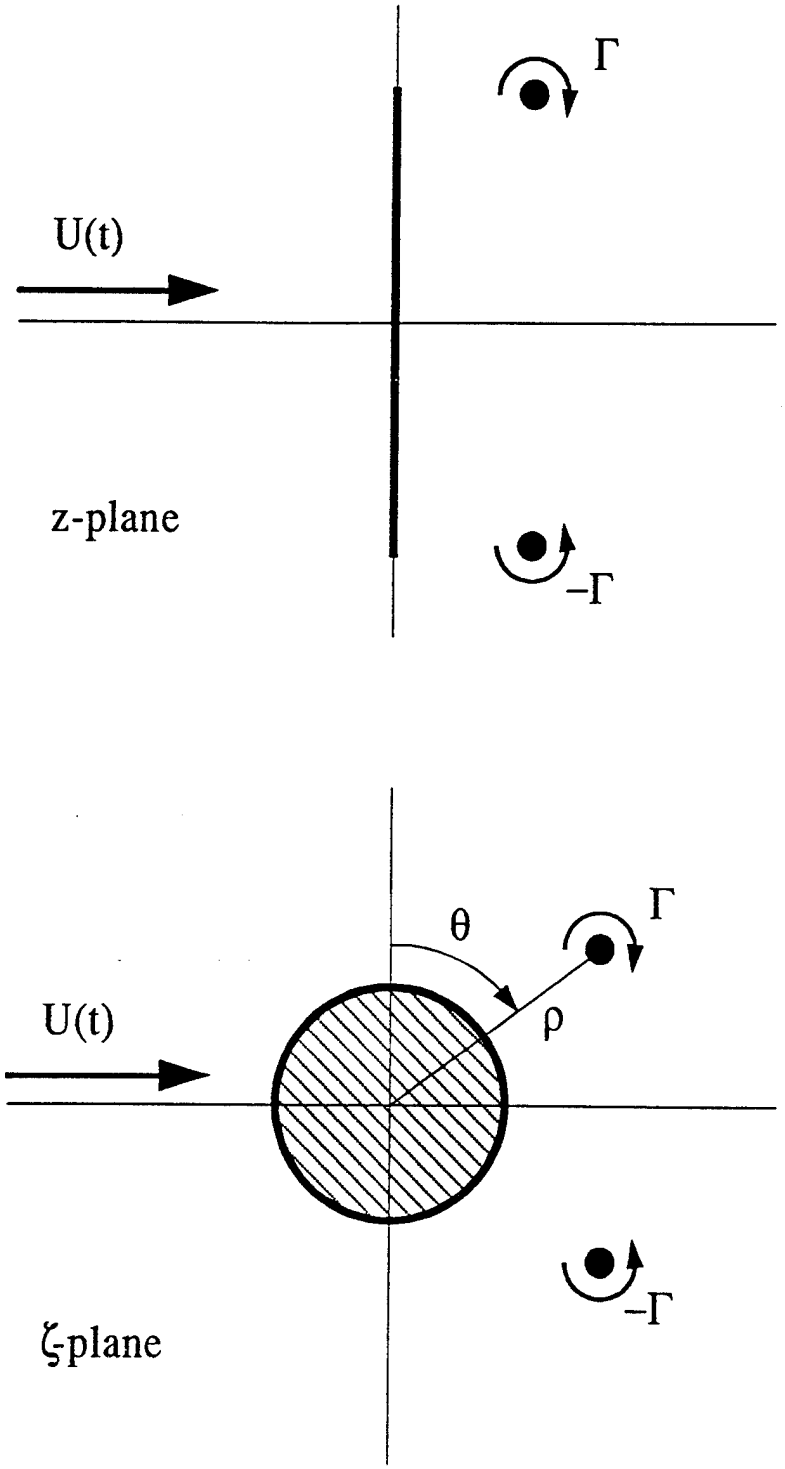

Figure 1: Physical and mapped planes for the flow past a flat plate.

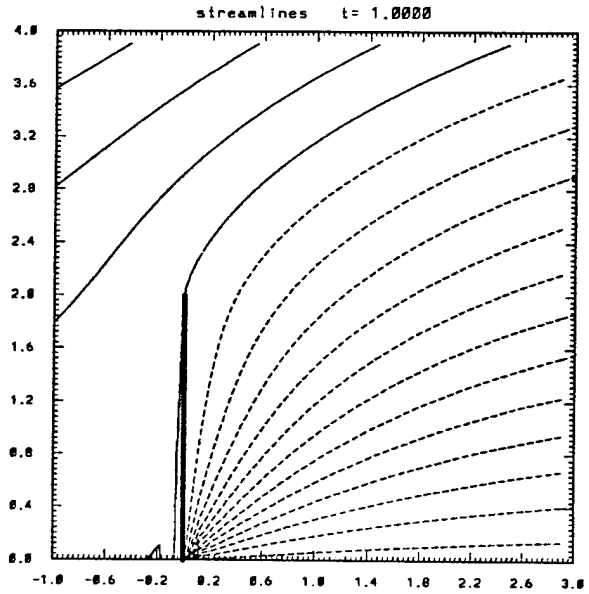

Figure 2: Instantaneous streamlines, $s = -2U$.

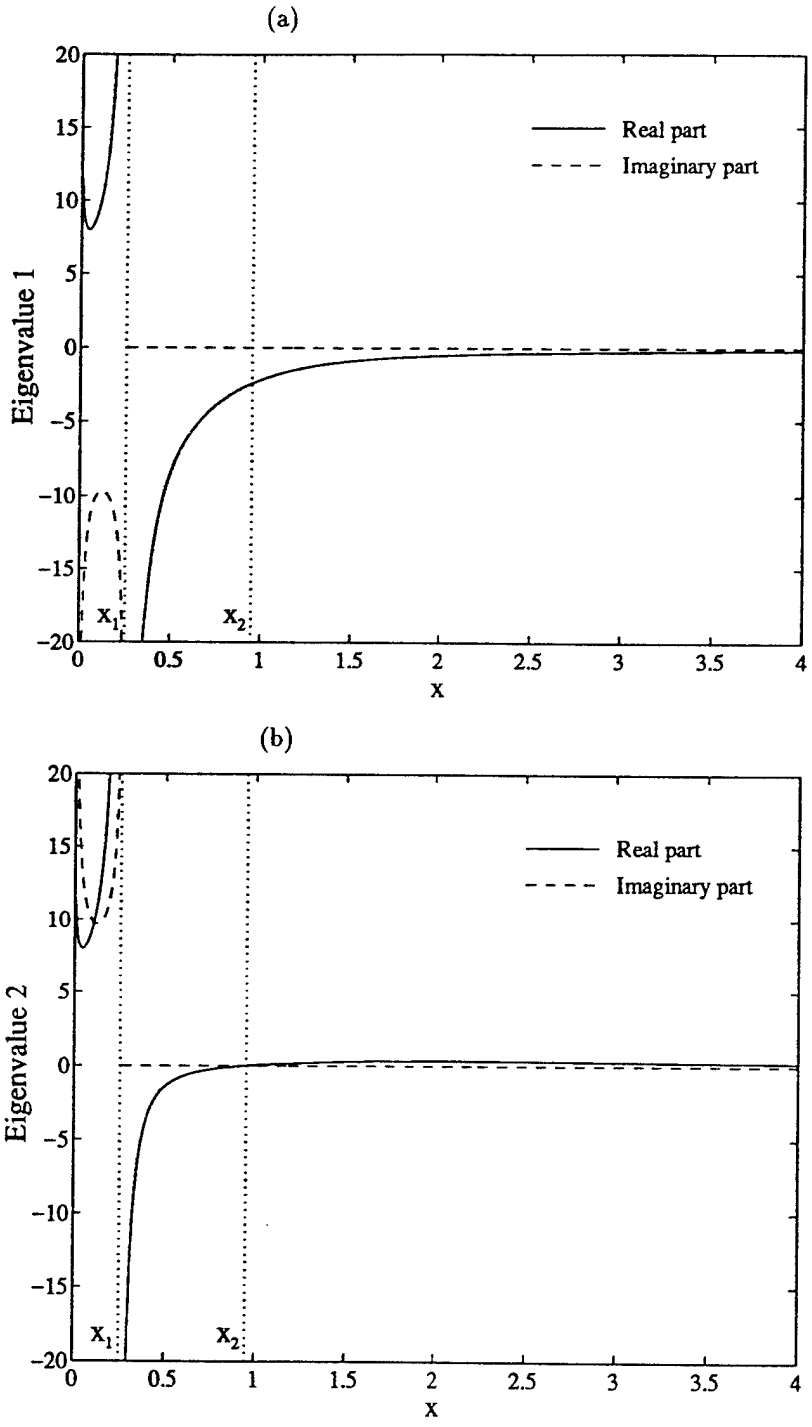

Figure 3: Real and imaginary parts of the eigenvalues λ_1 (a) and λ_2 (b).

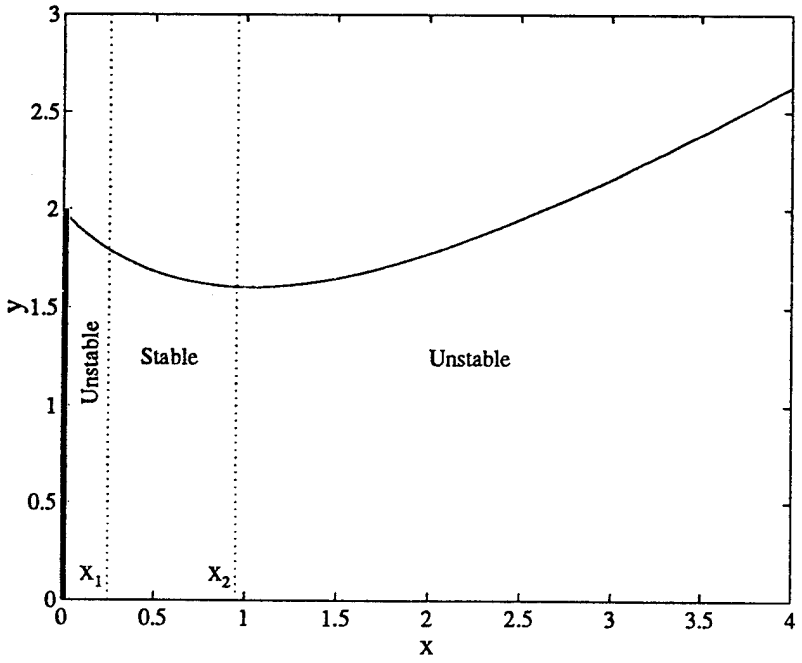

Figure 4: Locus of the fixed points.

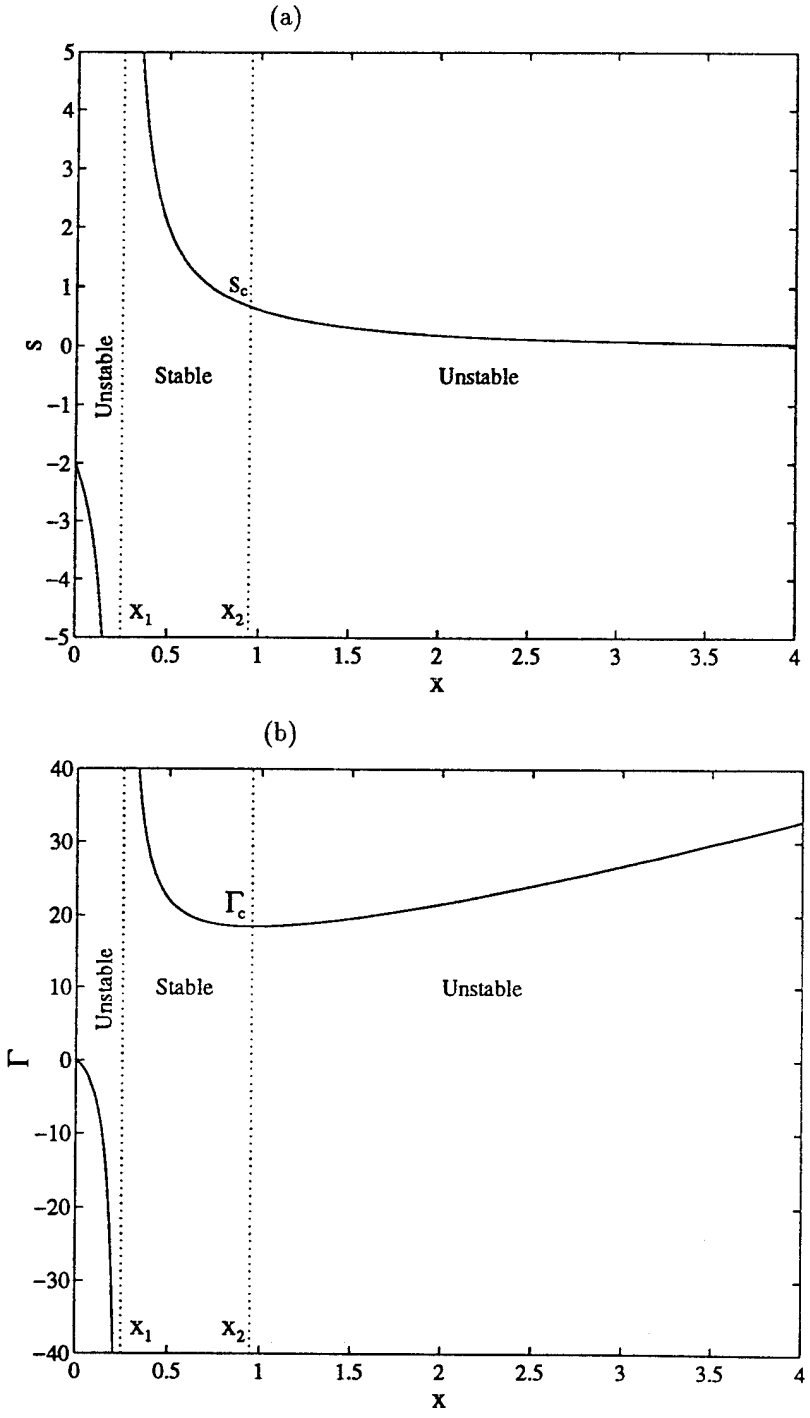

Figure 5: Suction (a) and circulation of the top vortex (b).

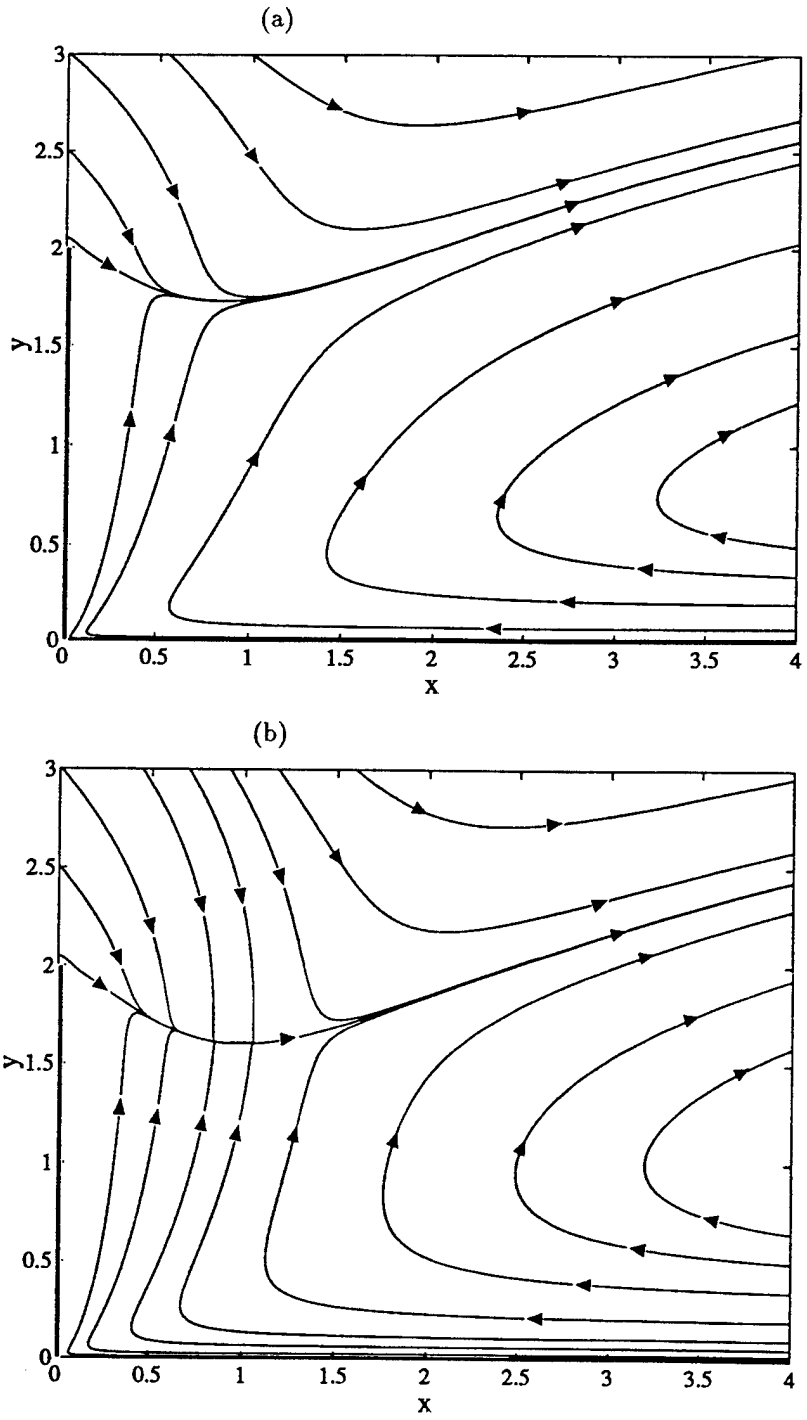

Figure 6: Vortex trajectories, $U = 1$: $\Gamma_{1_s} = 15$ (a), $\Gamma_{1_s} = 18.49(b)$.

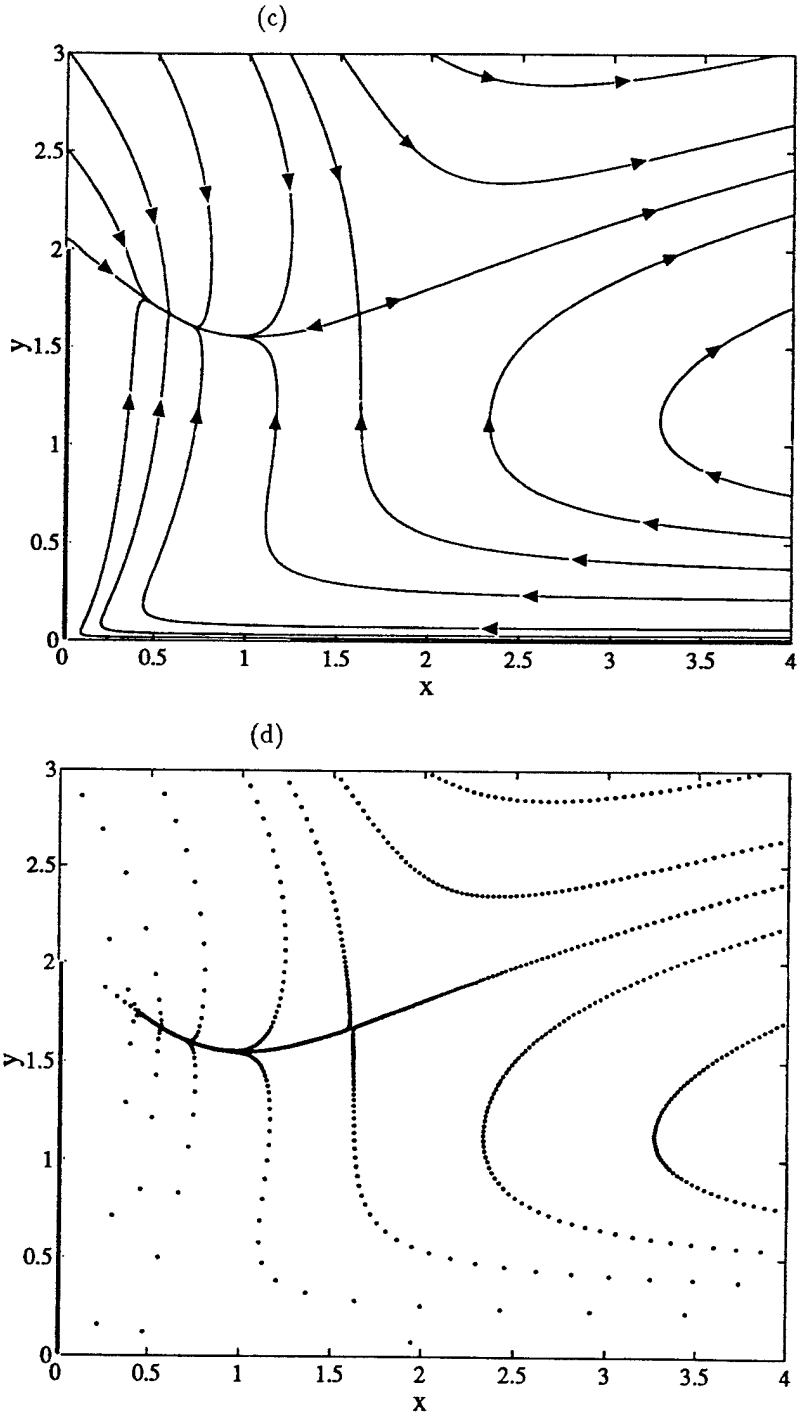

Figure 6: (Continued) Vortex trajectories, $U = 1$, $\Gamma_{1_s} = 20$ (c); Poincaré section, $U = 1 + \epsilon \sin(\omega t)$, $\epsilon = 0.1$, $\omega = 20\pi$, $\Gamma_{1_s} = 20$ (d).

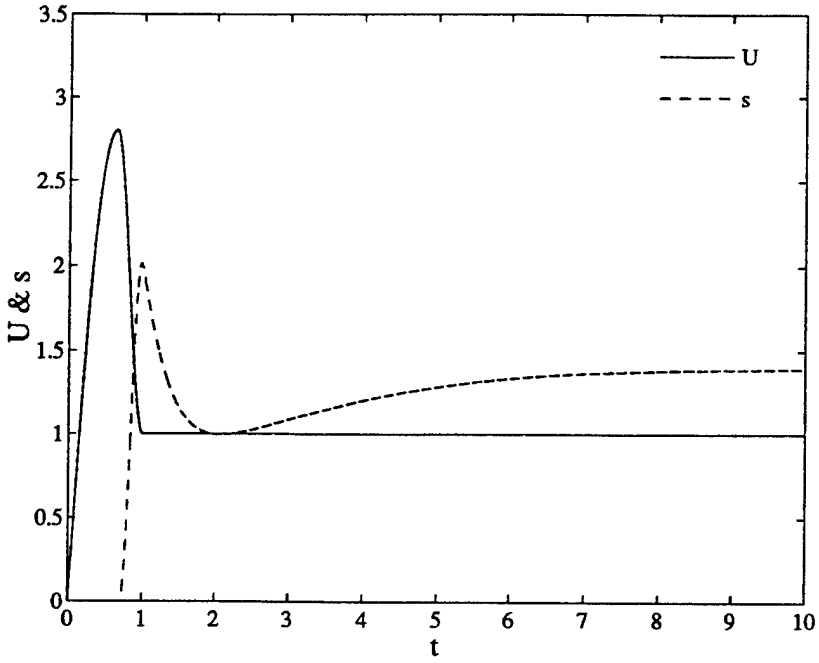

Figure 7: Free-stream velocity and suction.

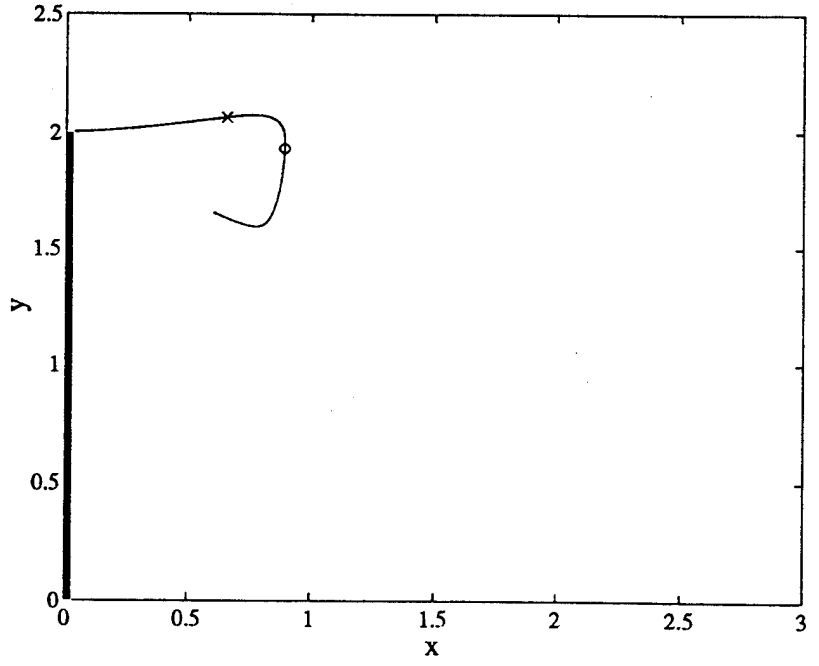

Figure 8: Trajectory of the top vortex, (×) vortex position at $t = t_s$, (o) vortex position at $t = 1$.

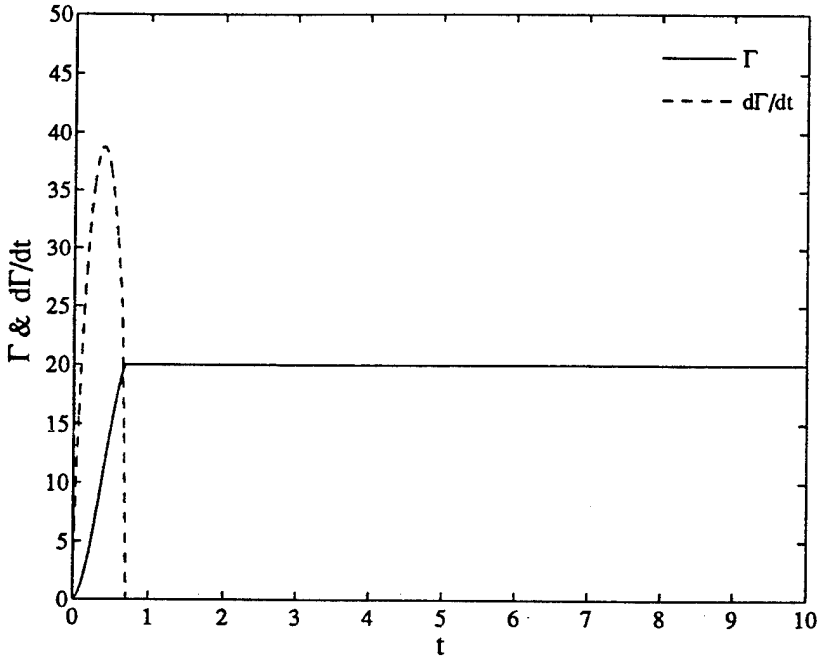

Figure 9: Circulation and rate of circulation production associated with the top vortex.

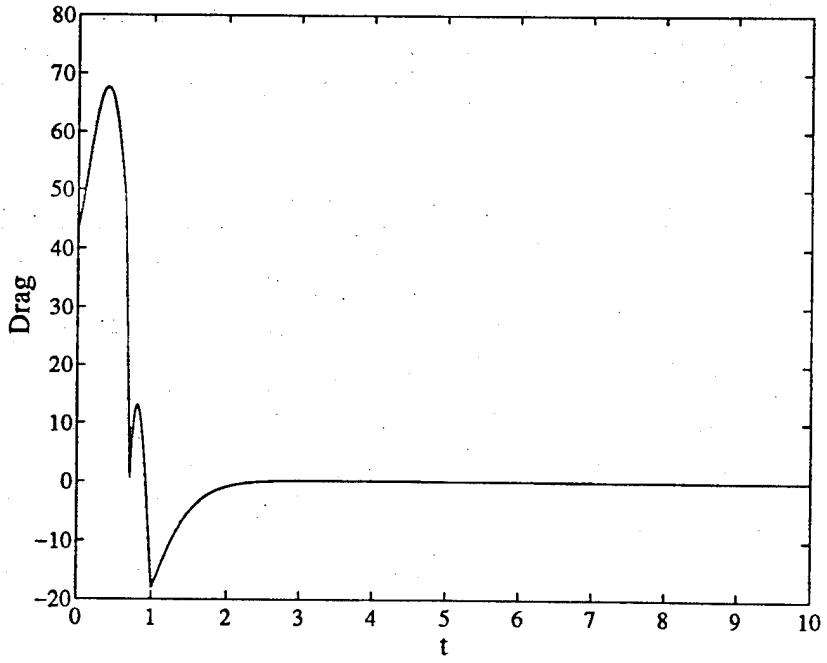

Figure 10: Drag.

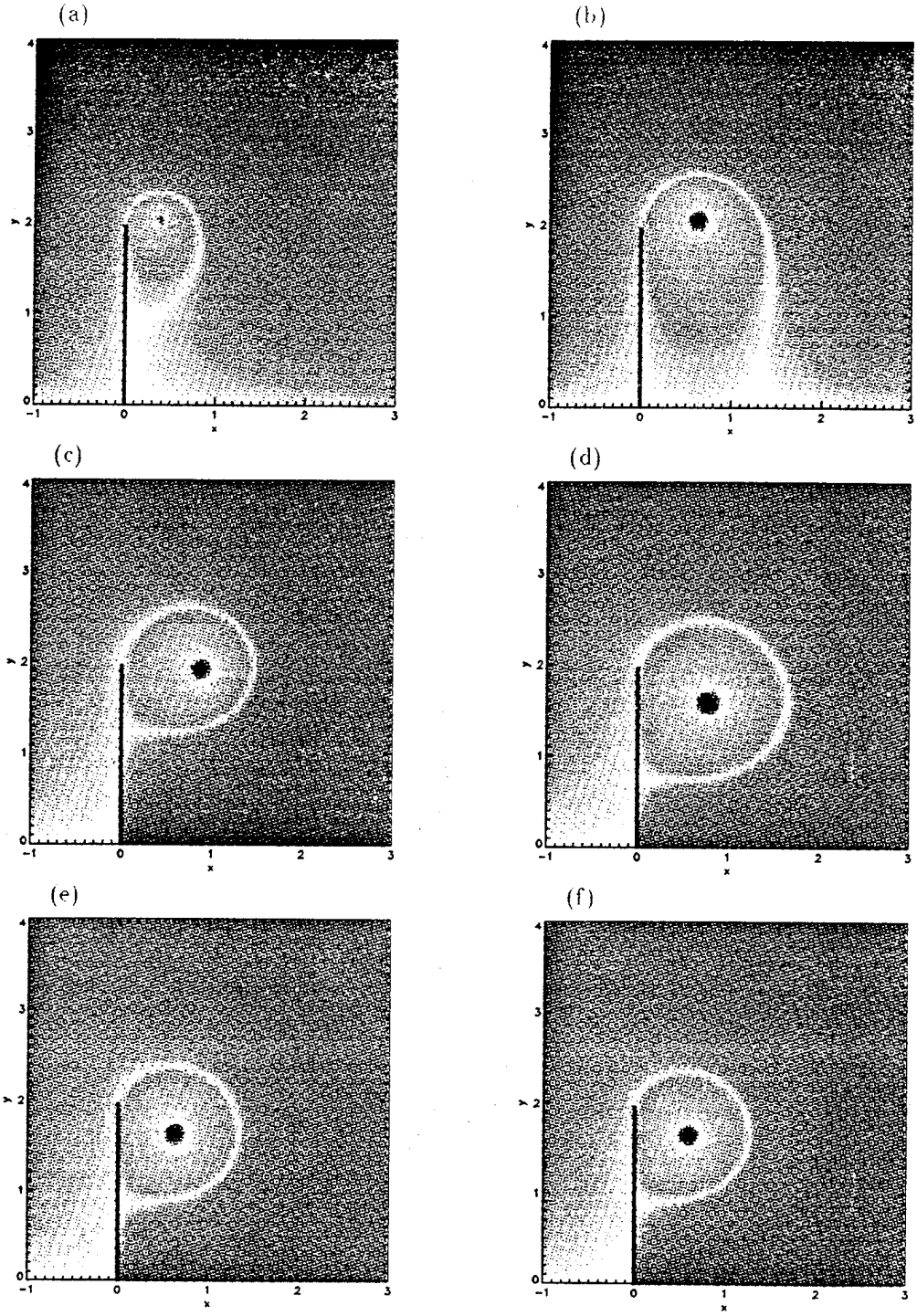

Figure 11: Instantaneous streamlines, t=0.51(a), t=1.02(b), t=2.02(c), t=4.02(d), t=6.02(e), t=8.02(f).

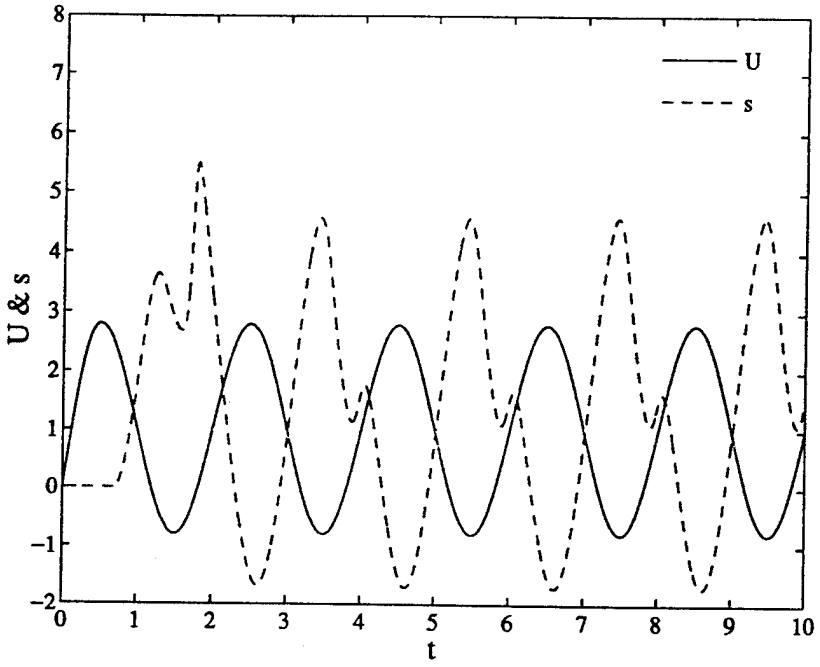

Figure 12: Free-stream velocity and suction.

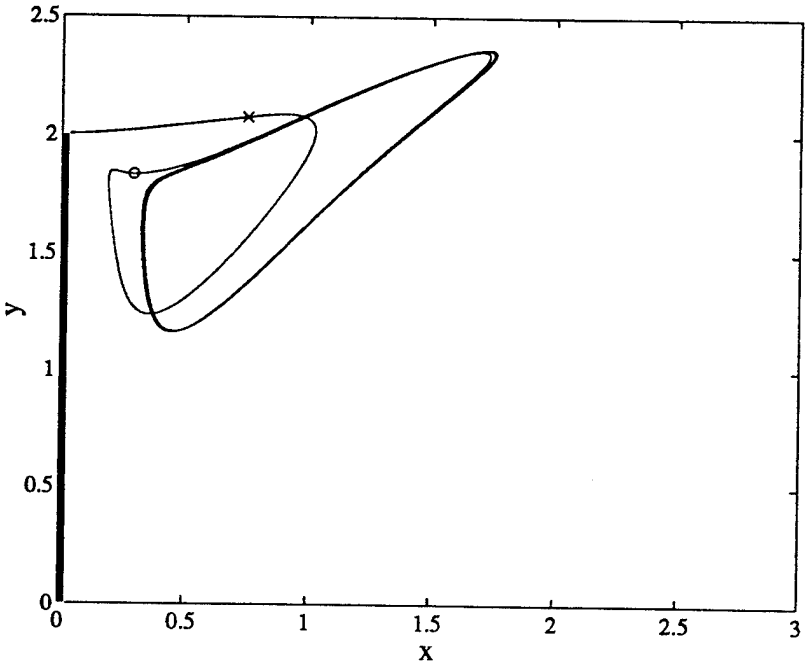

Figure 13: Trajectory of the top vortex, (×) vortex position at $t = t_s$, (o) vortex position after one period, $t = 2$.

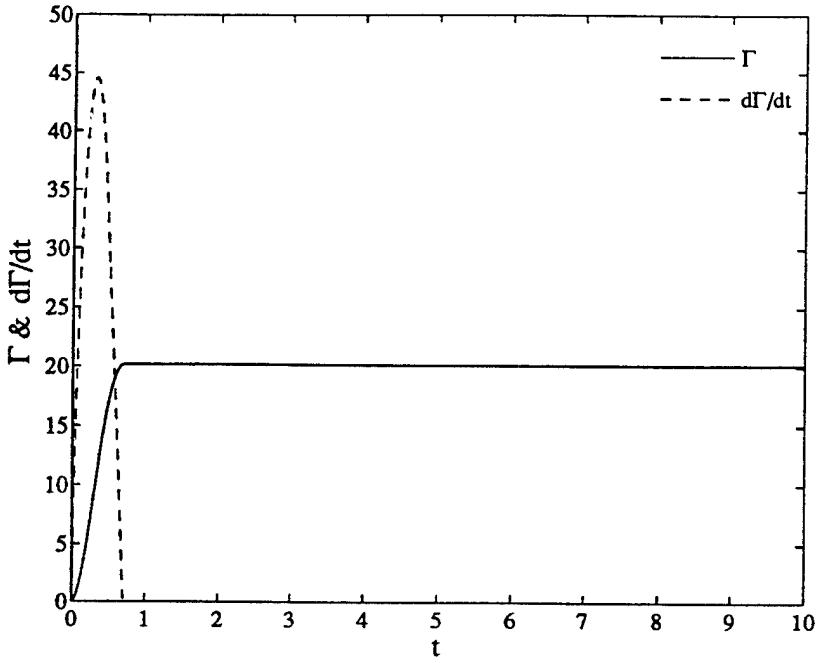

Figure 14: Circulation and rate of circulation production associated with the top vortex.

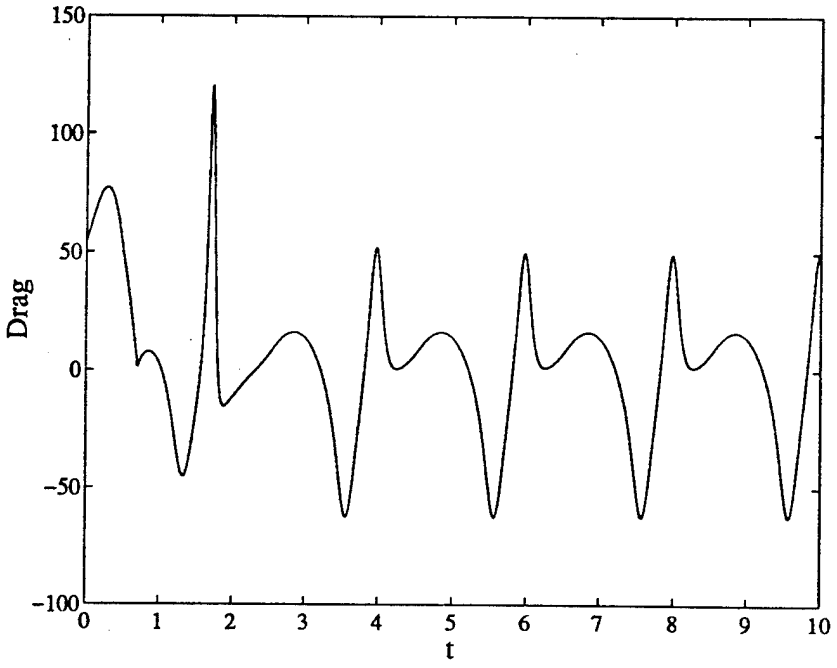

Figure 15: Drag.

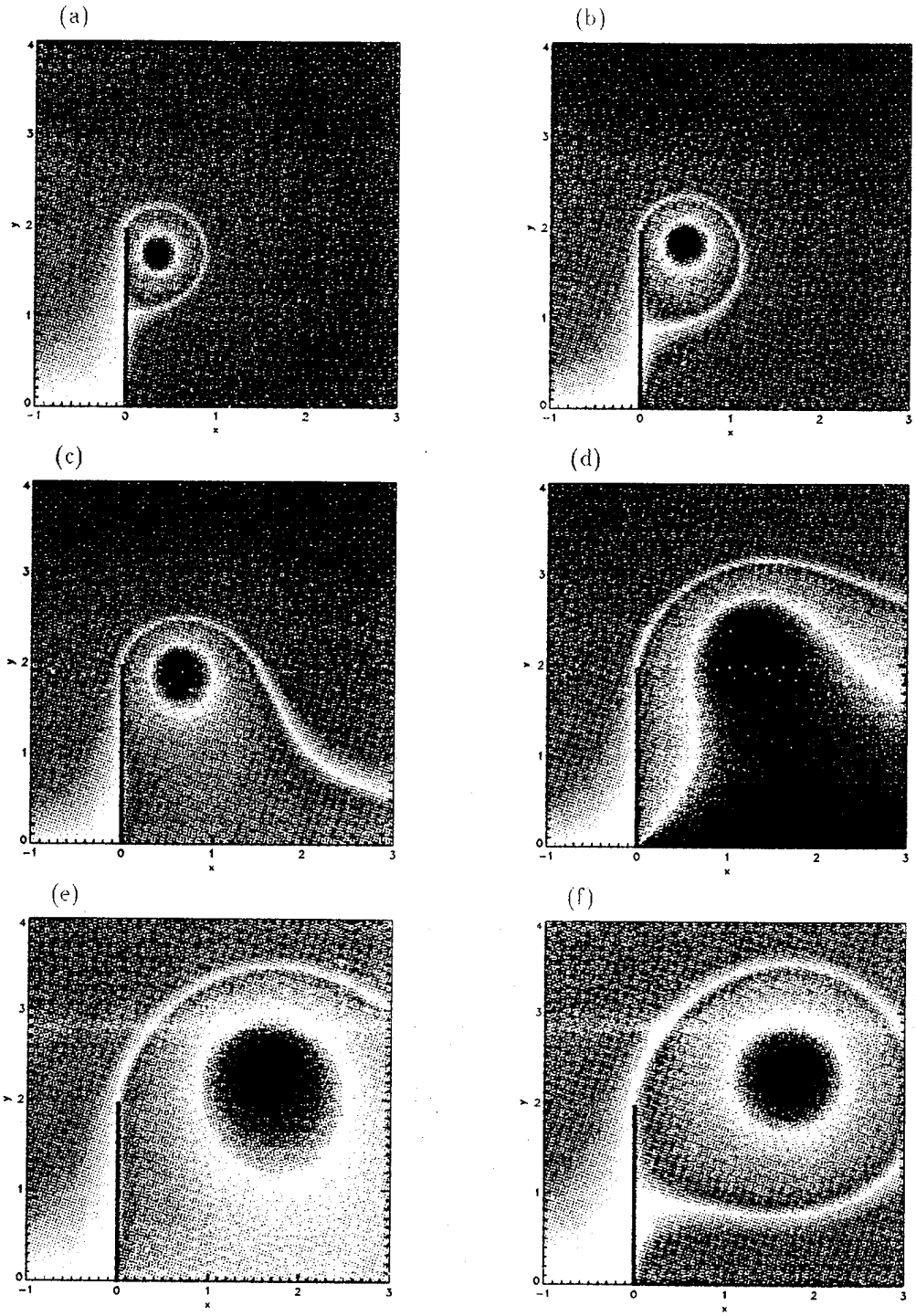

Figure 16: Instantaneous stream fuction, t=6.05(a), t=6.25(b), t=6.35(c), t=6.66(d), t=6.86(e), t=6.96(f).

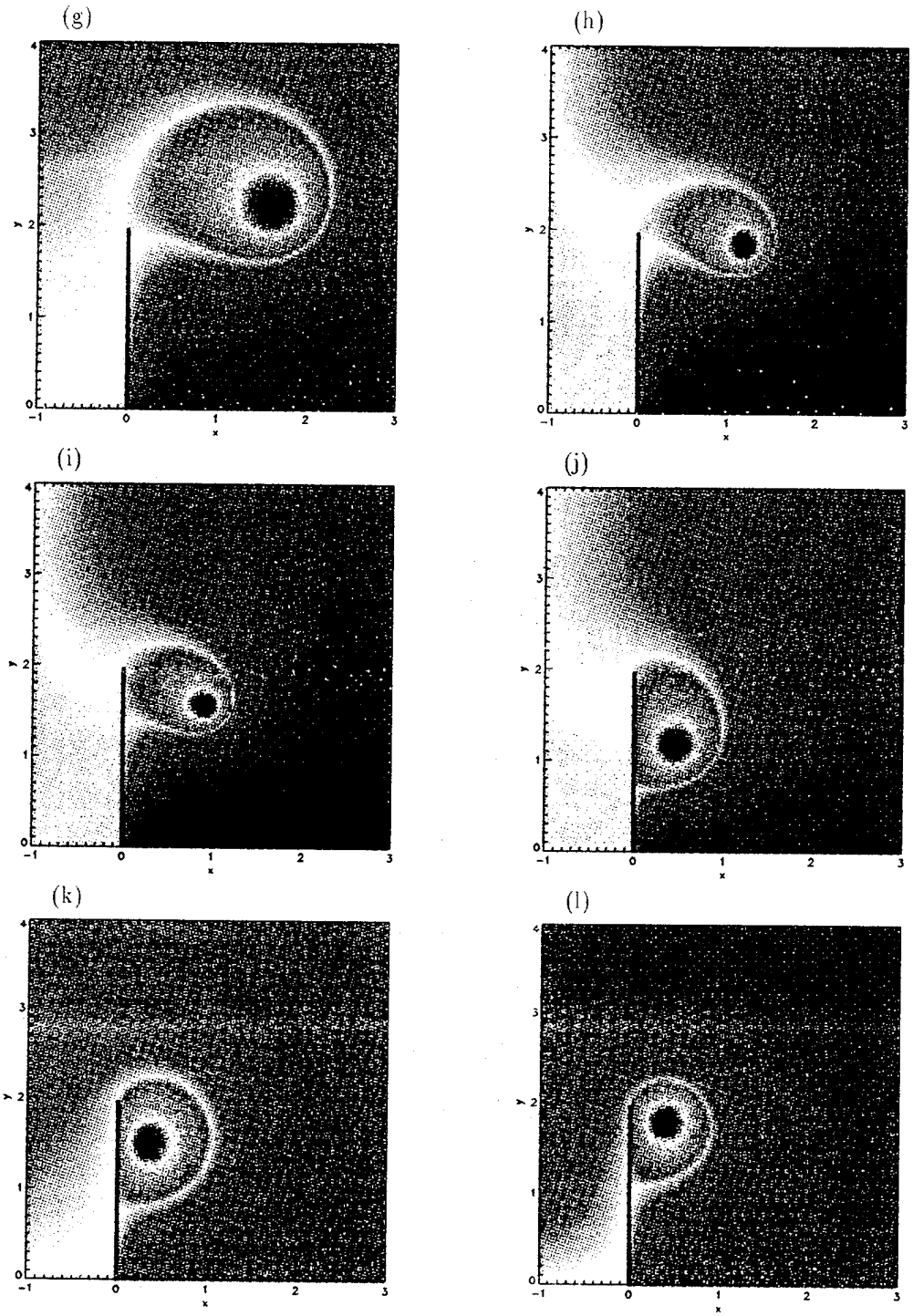

Figure 16: (Continued) Instantaneous stream function, t=7.16(g), t=7.36(h), t=7.46(i), t=7.67(j), t=7.87(k), t=8.07(l).

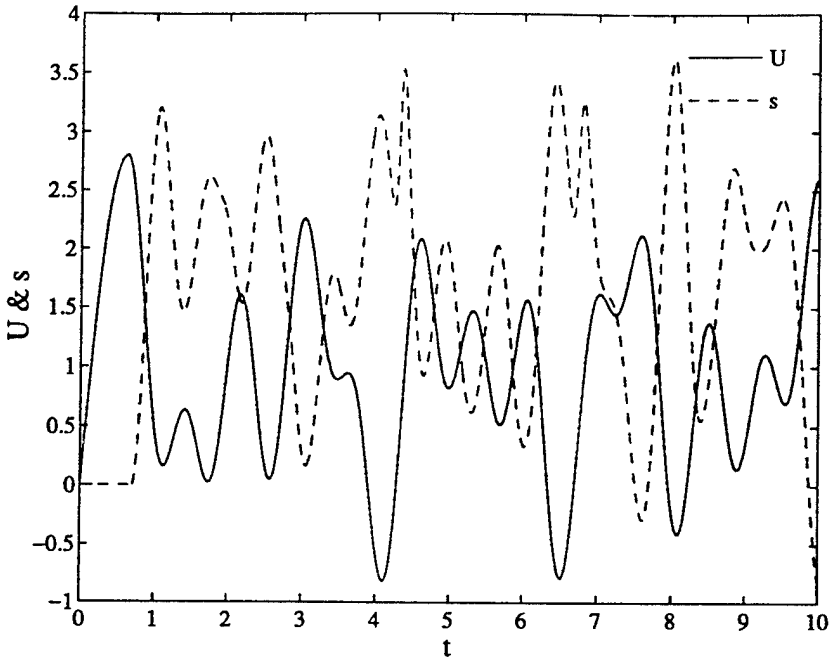

Figure 17: Free-stream velocity and suction.

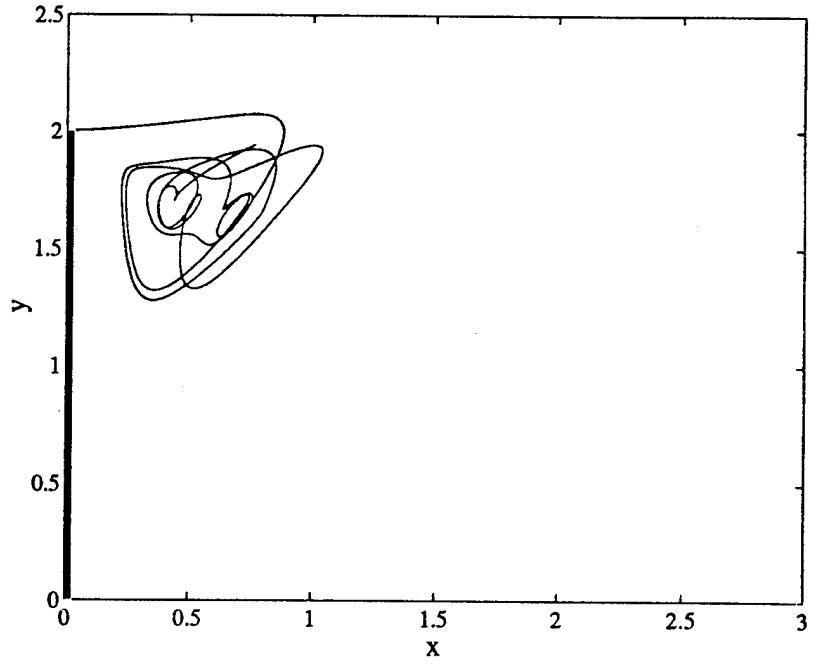

Figure 18: Trajectory of the top vortex.

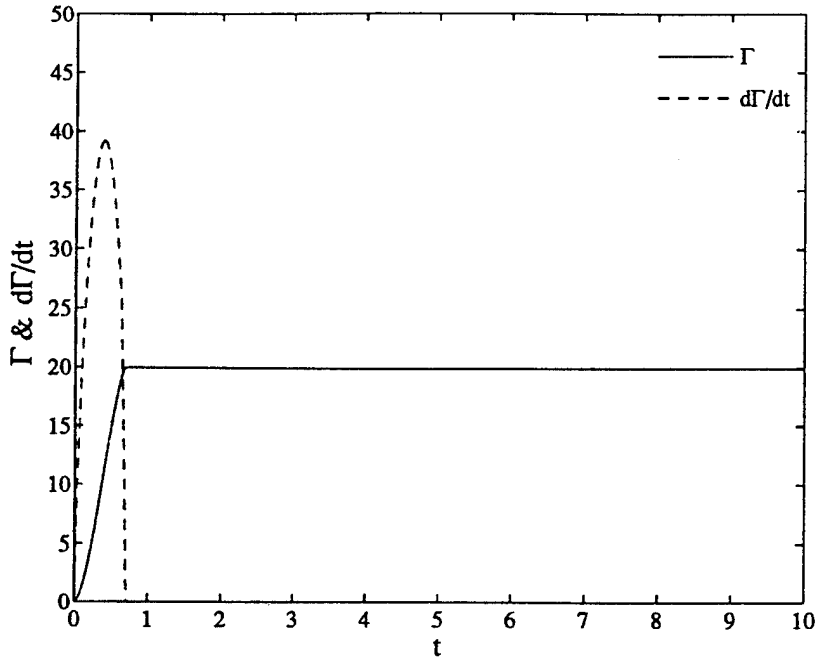

Figure 19: Circulation and rate of circulation production associated with the top vortex.

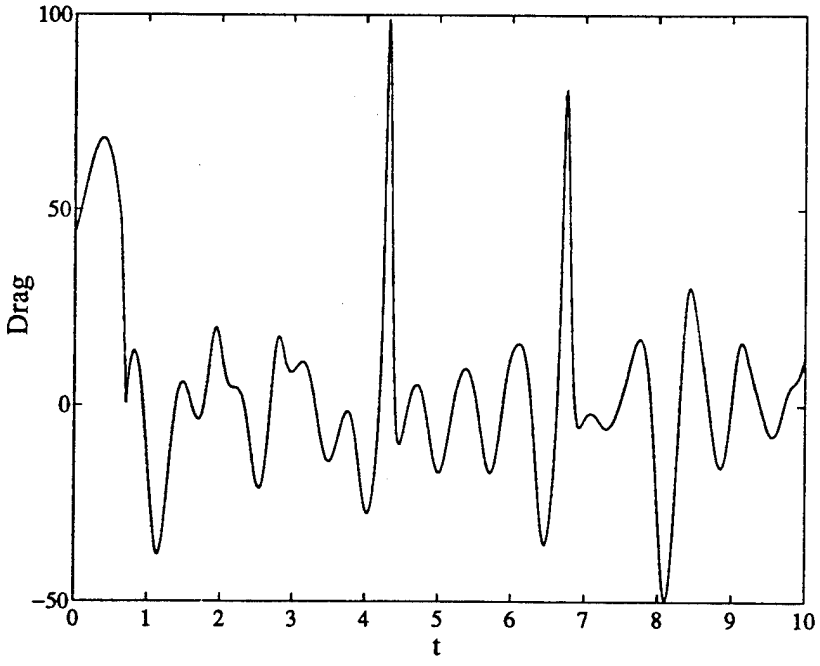

Figure 20: Drag.

References

Brown, C.E. & Michael, W.H. 1954 Effect of leading-edge separation on the lift of a delta wing. *J. Aero. Sci.* **21**, 690–694.

Cao, N-Z & Aubry, N. 1993 Numerical simulation of a wake flow via a reduced system. FED-Vol. 149, Separated flows, ASME 1993

Cheers, A.Y. 1979 A study of incompressible 2-d vortex flow past a circular cylinder. Lawrence Berkeley Laboratory LBL-9950.

Clements, R.R. 1973 An inviscid model of two-dimensional vortex shedding. *J. Fluid Mech.* **57**, 321–336.

Cortelezzi, L., Leonard, A. & Doyle, J.C. 1994 An example of active circulation control of the unsteady separated flow past a semi-infinite plate. *J. Fluid Mech.* **260**, 127–154.

Cortelezzi, L. 1995 A reduced model for the unsteady separated flow past a plate perpendicular to the free-stream velocity. To be submitted to: *Fluid Dynamic Research*

Doyle, J.C. Francis, B.A. & Tannenbaum, A.R. 1992 Feedback control theory. The Macmillan Company, New York

Fan, M.K.H. Tits, A.L. & Doyle, J.C. 1991 Robustness in the presence of mixed parametric uncertainty and unmodeled dynamics. *IEEE Auto. C.* **36**, 25–38.

Gad-el-Hak, M. & Bushnell, D.M. 1991 Separation control: review. *ASME J. Fluids Eng.* **113**, 5–30.

Graham, J.M.R. 1980 The forces on the sharp-edged cylinders in oscillatory flow at low Keulegan-Carpenter numbers. *J. Fluid Mech.* **97**, 331–346.

Gopalkrishnan, R., Triantafyllou, M.S., Triantafyllou, G.S. & Barrett, D 1994 Active vorticity control in a shear flow using a flapping foil. *J. Fluid Mech.* **274**, 1–21.

Guckenheimer, J. & Holmes, P. 1983 Nonlinear oscillations, dynamical systems, and bifurcation of vector fields. Springer-Verlag, New York

Koochesfahani, M.M. & Dimotakis, P.E. 1988 A cancelation experiment in a forced turbulent shear layer. *First National Fluid Dynamics Congress July 25-28, 1988, Cincinnati, Ohio.* AIAA Paper No. 88-3713-CP.

Lisoski, D.L. 1993 Nominally 2-dimensional flow about a normal flat plate. Ph.D. Thesis, California Institute of Technology.

Ongoren, A. & Rockwell, D. 1988a Flow structure from an oscillating cylinder Part 1. Mechanisms of phase shift and recovery in the near wake. *J. Fluid Mech.* **191**, 197–223.

Ongoren, A. & Rockwell, D. 1988b Flow structure from an oscillating cylinder Part 2. Mode competition in the near wake. *J. Fluid Mech.* **191**, 225–245.

Rajaee, M., Karlsson, S.K.F. & Sirovich, L. 1994 Low-dimensional description of free-shear-flow coherent structures and their dynamical behavior. *J. Fluid Mech.* **258**, 1–29.

Rao, D.M. 1987 Vortical flow management techniques. *Prog. Aerospace Sci.* **24**, 173–224.

Rossow, V.J. 1977 Lift enhancement by an external trapped vortex. *10th Fluid and Plasmadynamics Conference, June 27-29, 1977, Albuquerque, New Mexico.* AIAA Paper No. 77-672.

Roussopoulos, K. 1993 Feedback control of vortex shedding at low Reynolds numbers. *J. Fluid Mech.* **248**, 267–296.

Slomski, J.F. & Coleman, R.M. 1993 Numerical simulation of vortex generation and capture above an airfoil. *31st Aerospace Sciences Meeting and Exhibit, January 11-14, 1993, Reno. Nevada.* AIAA Paper No. 93-864.

Tokumaru, P.T. & Dimotakis, P.E. 1991 Rotary oscillation control of a cylinder wake. *J. Fluid Mech.* **224**, 77–90.

Adaptive Control of Vortex Dynamics *

C.R. Anderson
Department of Mathematics
University of California
Los Angeles, CA 90024-1555

H.-L. Chang and J.S. Gibson
Mechanical, Aerospace and Nuclear Engineering
University of California
Los Angeles, CA 90024- 1597

Abstract

An adaptive controller is used to reduce the oscillation of the cross-stream velocity at a point on the center line of an oscillating wake behind two vortex sources. The flow field is simulated by a new finite vortex street model, which uses discrete vortex blobs to model the vortex dynamics of the fluid flow.

1 Introduction

Discrete vortex models have been used to simulate many fluid-flow phenomena, including flow past bluff bodies and vortex sound generation [6, 2, 4, 1]. In this paper, a two-source vortex street model [3] is used to simulate an oscillating wake typical of many flows.

An adaptive LQG controller is used to reduce the oscillation of the cross-stream velocity measured at a point on the center line of the flow field. The controller is based on a linear digital input/output model of the flow, even though the vortex simulation is highly nonlinear. The control philosophy is to allow the parameters in the linear control model to vary adaptively to identify a local linearization of the true nonlinear input/output model. The adaptive controller uses a new adaptive QR algorithm for numerically stable and efficient parameter estimation.

2 Vortex Model

Suppose that there are N vortices located at (x_i, y_i) for $i = 1, \cdots, N$. The dynamical equations of the vortex model are

$$\frac{dx_i}{dt} = U_i(t) = U_p(x_i, y_i) + \frac{1}{2\pi} \sum_{j=1, j\neq i}^{N} \frac{\Gamma_j (y_j - y_i)}{((x_i - x_j)^2 + (y_i - y_j)^2)}, \quad (1)$$

$$\frac{dy_i}{dt} = V_i(t) = V_p(x_i, y_i) + \frac{1}{2\pi} \sum_{j=1, j\neq i}^{N} \frac{\Gamma_j (x_i - x_j)}{((x_i - x_j)^2 + (y_i - y_j)^2)}, \quad (2)$$

where Γ_i is vorticity strength of the i^{th} vortex and $U_p(x_i, y_i)$ and $V_p(x_i, y_i)$ are the velocities from potential flow. The part of the velocity field due to potential flow is taken to be $U_p = 1.0$ and $V_p = 0$ to represent a constant, uniform free-stream velocity. New vortices are generated in pairs from two vortex sources at $(0.0, \pm 0.5)$ with opposite vorticity $\pm\Gamma_i$. The series of vortices generated form the wake-like vortex street and roll up down stream of the vortex sources. To maintain a fixed number of vortices after a short start-up period, each vortex strength Γ_i fades to zero after N time steps [3, 5]. The vortex roll-up formed with $N = 150$ and Γ_i equal to the same constant Γ for all vorticies (before fading) is shown in Figure 1.

For the control problem, the measured and controlled output is the vertical velocity V_0 at the fixed point $(0.0, 0.0)$ (i.e., the midpoint between the two vortex sources). This velocity component is given by

$$V_0(t) = \frac{1}{2\pi} \sum_{j=1}^{N} \frac{\Gamma_j (x_0 - x_j)}{((x_0 - x_j)^2 + (y_0 - y_j)^2)}. \quad (3)$$

The control action is the variation Γ_u of the strength of the newly generated vortices. Thus, at the time step when a pair of vortices is introduced at the sorces, the strengths of the two new vortices, respectively,

$$\Gamma_{new} = \pm\Gamma + \Gamma_u \quad (4)$$

where Γ is a constant nominal strength.

3 Adaptive Controller

Rather than base the controller design on the large number (300 in the example here) of coupled nonlinear differential equations governing the vortex dynamics, the approach presented here uses a linear input-output model with time-varying coefficients as the basis of the control design. This ARX model is

$$y(t) = -\sum_{i=1}^{N} a_i(t) y(t-i) + \sum_{j=1}^{N} b_j(t) u(t-j). \quad (5)$$

*This research was supported by AFOSR Grant F49620-92-J-0279.

where the output $y(t)$ is the vertical velocity $V_0(t)$, the control $u(t)$ is the perturbation Γ_u in the strenth of the two vortices introduced at time t, and $a_i(t)$ and $b_j(t)$ are the time-varying coefficients. These coefficients are estimated adaptively by an adaptive QR algorithm, and the parameter estimates at each time t are used to update the gains in an adaptive *LQG* controller.

4 Simulation Results

When the system is initialized with a single vortex, the cross-stream velocity at the point half way between the two vortex sources approaches the steady-state oscillation shown in Figure 2. The controlled output is shown in Figure 3. Before the feedback control loop is closed at time step 420, a known random input sequence u of small amplitude forces the system to provide input-output data for initial parameter estimation. The feedback controller reduces the output amplitude to about 10% of the open-loop amplitude.

It is common for nonlinear systems to have different frequencies of oscillation for different amplitudes. For the system studied here, the amplitude of the output signal is reduced by the controller, and the closed-loop response has frequencies that were not significant in the open-loop response. Thus, the parameters in the controller must be reidentified after the control loop is closed. The results here indicate that, by changing the parameters adaptively, the controller can maintain a significant reduction in output amplitude.

References

[1] Christopher Anderson and Claude Greengard. On vortex methods. *SIAM Journal of Numerical Analysis*, 22(3):413–440, June 1985.

[2] R. R. Clements. An invisid model of two-dimensional vortex shedding. *Journal of Fluid Mechanics*, 57:321–336, 1973.

[3] C.R. Anderson. *A Finite Vortex Street Model.* Technical Report 93-01, UCLA, 1993.

[4] T. Kambe. Acoustic emissions by vortex motion. *Journal of Fluid Mechanics*, 173:643–666, 1986.

[5] Reiyu Chein and J. N. Chung. Discrete-vortex simulation of flow over inclined and normal plates. *Computers and Fluids*, 405–427, 1988.

[6] Turgut Sarpkaya and Ray L. Schoaff. Inviscid model of two-dimensional vortex shedding by a circular cylinder. *AIAA Journal*, 17(11):1193–1200, 1979.

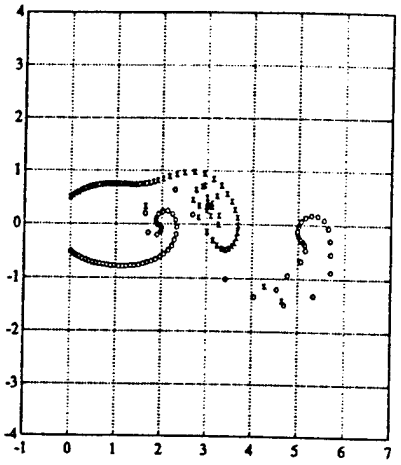

Figure 1: Vortex distribution for $N = 150$

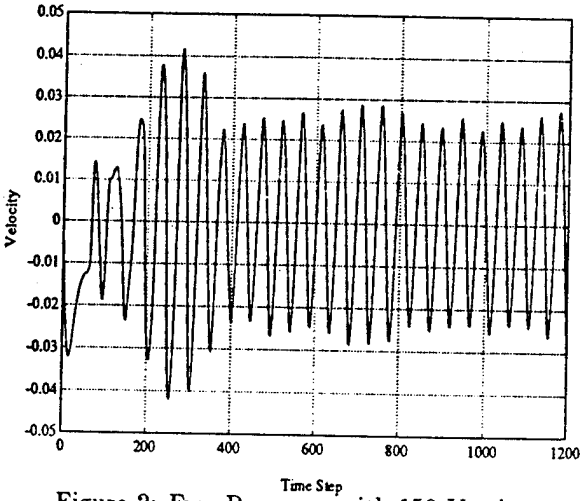

Figure 2: Free Response with 150 Vortices

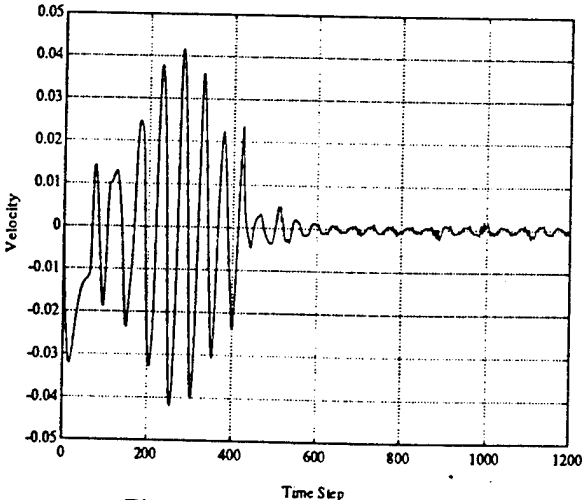

Figure 3: Controlled Response

Zeros of Input/Output Models for Control of Vortex Dynamics [1]

C.R. Anderson
Department of Mathematics
University of California
Los Angeles, CA 90024-1555

H.-L. Chang and J.S. Gibson
Mechanical, Aerospace and Nuclear Engineering
University of California
Los Angeles, CA 90024-1597

Abstract

This paper studies the zeros of input/output models used in controlling the oscillating wake behind two vortex sources. The numerical results presented show that the stability of the zeros of adaptively identified input/output models depends on whether the sensors are upstream or downstream of the actuator.

1. Introduction

Discrete vortex models have been used to simulate many fluid-flow phenomena, including flow past bluff bodies and vortex sound generation [1, 5]. In this paper, a two-source vortex street model is used to simulate an oscillating wake typical of many flows [4].

In [2, 3], an adaptive LQG controller is used to reduce the oscillation of the cross-stream velocity measured at a point on the center line of the flow field. The controller is based on a linear digital input/output model of the flow, even though the vortex simulation is highly nonlinear. The control philosophy is to allow the parameters in the linear control model to vary adaptively to identify a local linearization of the true nonlinear input/output model. The adaptive controller uses an adaptive QR algorithm for numerically stable and efficient parameter estimation.

The LQG controller used in [2, 3] works well as long as the position at which the cross-stream velocity is measured and controlled is not downstream of the actuator. Whenever the measurement point is downstream of the actuator, the feedback control command goes unstable. This suggests two possibilities: either the adaptively varying linear input/output model used for the controller does not approximate the dynamics of the flow sufficiently when the sensor is downstream of the actuator, or the actual nonlinear vortex model possesses unstable zero dynamics when the sensor is downstream of the actuator.

[1] This research was supported by AFOSR Grant F49620-92-J-0279.

We have investigated the zero dynamics of the vortex model in two ways. First, we used an adaptive QR algorithm to identify linear input/output (ARX) models of various orders from input/output data, as in [2, 3]. Second, we implemented a nonlinear one-step-ahead contoller based on the explicit vortex model (i.e., the nonlinear simulation simulation model). We considered both the single-input/single-output case and the single-input/two-output case where two sensors measure cross-stream velocities at different points on the center line of the flow field.

The adaptively identified ARX models consistently exhibit stable zeros when the sensors are upstream of the actuator but unstable zeros when the sensors are downstream of the actuator. In simulations, the nonlinear controller—applied to the exact simulation model for which it was designed—drives the output close to zero with a bounded control signal when the sensors are upstream of the actuator, but the control signal generated by the nonlinear one-step-ahead contoller goes unstable whenever sensors are downstream of the actuator. The performance of the nonlinear controller, which is based on the explicit vortex dynamics, indicates that, indeed, the stability of the zero dyanics of the nonlinear flow depends on whether the sensors are upstream or downstream of the actuator, and the adaptively identified input/output models correctly capture this property, which is important for feedback control.

2. Vortex Model

Suppose that there are N_v vortices, with the k^{th} vortex located at the point z_k $(k = 1, \cdots, N_v)$ in the complex plane. The equations of motion for the vortex model are

$$\frac{d\bar{z}_k}{dt} = \bar{U}_p(z_k) + \frac{1}{2\pi i} \sum_{j=1, j\neq k}^{N_v} \frac{\Gamma_j}{z_k - z_j}, \qquad (1)$$

where Γ_k is circulation of the k^{th} vortex and $U_p(z_k)$ is the complex velocity from potential flow. The part of the velocity field due to potential flow is taken to be $U_p = 1.0$ to represent a constant, uniform free-stream velocity. New vortices are generated in pairs from two vortex sources at $(0.0, \pm 0.5)$ with opposite vorticity $\pm\Gamma_k$. The series of vortices generated form a wake-like vortex street and roll up down stream of the vortex sources.

For the control problem, each measured and controlled output is the vertical velocity at a fixed point $(x, 0.0)$ (i.e., a point located a distance x along the horizontal center line between the two vortex sources) Upstream means $x < 0$; downstream means $x > 0$. The control action is the variation Γ_u of the circulation of the newly generated vortices. At the time step when a pair of vortices is introduced at the sorces, the circulations of the two new vortices, respectively,

$$\Gamma_{new} = \pm\Gamma + \Gamma_u \qquad (2)$$

where Γ is a constant nominal circulation. Hence, the control actuator is located at $x = 0$.

3. The Adaptively Identified Input/Output Model and Its Zeros

The input/output model has the form

$$y(t) = -\sum_{j=1}^{N} A_j(t)y(t-j) + \sum_{j=1}^{N} B_j(t)u(t-j) \qquad (3)$$

where $y(t)$ is the vector of measured vertical velocities, the scalar control is $u = \Gamma_u$. For the results presented in this paper, vertical velocities at two points are measured, so each $A_i(t)$ is a 2×2 coefficient matrix, and each $B_j(t)$ is a 2×1 vector. The system is forced with a known random input sequence u of small amplitude to generate input/output data for identification.

For one-step-ahead control and most other adaptive controllers, the relevant zeros are the roots to

$$B_1^T(t)\sum_{j=1}^{N} B_j(t)z^j = 0. \qquad (4)$$

The magnitudes of these zeros are plotted in Figures 1 and 2 for model order $N = 4$. We used two sets of locations for the two velocity sensors. The first set of sensor locations is $x = -1, -.5$ (both sensors upstream of the actuator). The second set of sensor locations is $x = +.5, +1$ (both sensors downstream of the actuator). The figures show that the identified zeros are all stable (magnitudes < 1) for the first set of sensor locations, but that one zero is unstable for the second set of sensor locations.

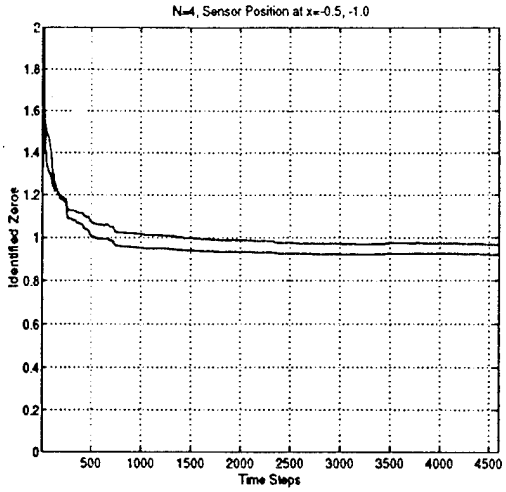

Figure 1: Identified Zeros for $N = 4$, Both Sensors Upstream

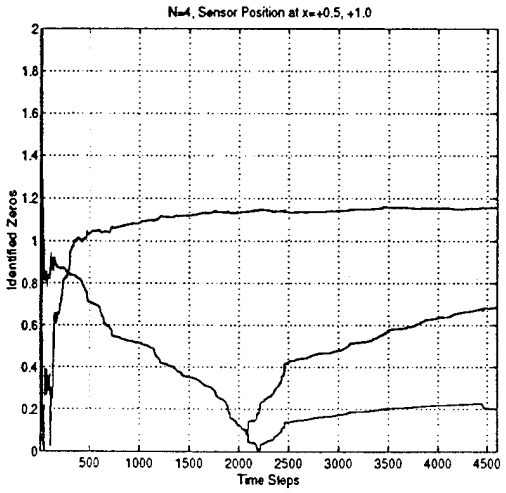

Figure 2: Identified Zeros for $N = 4$, Both Sensors Downstream

References

[1] C. R. Anderson, C. Greengard, and M. Henderson, editors. *Vortex Methods Lecture Notes in Mathematics.* Springer, 1988.

[2] C. R. Anderson, H.-L. Chang, and J. S. Gibson. Adaptive control of vortex dynamics. In *Conference on Decision and Control*, San Antonio, TX, December 1993. IEEE.

[3] H.-L. Chang. *Control of Vortex Dynamics.* PhD thesis, UCLA, March 1994.

[4] C.R. Anderson. A finite vortex street model. Technical Report 93-01, UCLA, 1993.

[5] Turgut Sarpkaya. Computational methods with vortices-the 1988 freeman scholar lecture. *Journal of Fluids Engineering*, 111:5–52, March 1989.